



Original article

2-Arylbenzofuran-based molecules as multipotent Alzheimer's disease modifying agents

Stefano Rizzo^{a,1}, Andrea Tarozzi^b, Manuela Bartolini^a, Gregory Da Costa^c, Alessandra Bisi^a, Silvia Gobbi^a, Federica Belluti^a, Alessia Ligresti^d, Marco Allarà^d, Jean-Pierre Monti^c, Vincenza Andrisano^a, Vincenzo Di Marzo^d, Patrizia Hrelia^b, Angela Rampa^{a,*}

^a Department of Pharmaceutical Sciences, Alma Mater Studiorum, University of Bologna, Via Belmeloro 6, 40126 Bologna, Italy

^b Department of Pharmacology, Alma Mater Studiorum, University of Bologna, Via Irnerio 48, 40126 Bologna, Italy

^c Laboratoire de Physique et Biophysique, GESVAB EA3675 ISVV, University of Bordeaux 2, 146 rue Léo Saignat, 33076 Bordeaux cedex, France

^d Endocannabinoid Research Group, Institute of Biomolecular Chemistry, National Research Council, Via Campi Flegrei 34, Comprensorio Olivetti, 80078 Pozzuoli, NA, Italy

ARTICLE INFO

Article history:

Received 20 August 2012

Received in revised form

11 October 2012

Accepted 26 October 2012

Available online 2 November 2012

Keywords:

Alzheimer's disease

2-Arylbenzofurans

Drug design

A β peptide

Neuroprotection

CB receptors

ABSTRACT

The complex etiology of Alzheimer's disease prompts scientists to develop multi-target strategies to combat causes and symptoms. In line with this modern paradigm and as a follow-up to our previous studies, we designed and synthesized a focused collection of new 2-arylbenzofurans and evaluated their biological properties towards specific targets involved in AD, namely human AChE and human BuChE, and A β fibril formation. Selected compounds were also tested for their ability to inhibit A β neurotoxicity in terms of neuronal viability loss, and to prevent A β peptide-binding to cell membrane and intracellular reactive oxygen species (ROS) formation. The different modifications introduced in the structure of our lead compound led to an increase in activity towards one or more of the selected targets: the anticholinesterase activity of some compounds was found to be significantly higher than previously obtained related molecules, and the compounds also proved to possess A β anti-aggregating properties and neuroprotective effects. The most interesting multi-target compounds were **18**, and **1**. Interestingly, **1** also showed good selectivity and moderate affinity for CB1 receptor, opening new perspectives in the field of research on AD, since cannabinoid ligands have been widely reported to have neuroprotective properties.

© 2012 Elsevier Masson SAS. All rights reserved.

1. Introduction

In the vast plethora of neurodegenerative disorders, Alzheimer's disease (AD) stands out as the most common form of dementia, afflicting more than 24 million of individuals worldwide. AD is characterized by an insidious onset and a chronic progression [1]. Symptoms worsen with the advancement of the disease, progressing from mild forgetfulness to widespread severe brain impairment. Although the highest peak of incidence occurs among elderly people (aged over 65, sporadic AD), cases of early onset have been also reported (5% of all cases) and are frequently associated with genetic predisposition (familial AD) [1]. Reflecting the world population ageing, the scenario is expected to worsen in the next

decades if no efficacious treatments is discovered that can stop the progression of the disease.

In AD brains, the cholinergic system is the most dramatically affected, showing remarkable depletion of acetylcholine (ACh) and other markers of the cholinergic activity (cholinergic hypothesis) [2]. Based on this observation, four drugs (tacrine, donepezil, rivastigmine, galantamine) have been approved by the FDA and are currently marketed for the symptomatic treatment of AD. Their mechanism of action is the inhibition of the active site of acetylcholinesterase (AChE), the enzyme responsible for the degradation of ACh, resulting in an increased level of the neurotransmitter in the synaptic cleft. Such a therapeutic strategy, though, exerts only palliative effects and does not stop the progression of the disease, indicating that the cholinergic impairment could be a downstream event of a more complex and multifactorial sequence, still not fully understood.

Two main neuropathological hallmarks are characteristically present in AD brains, namely intraneuronal neurofibrillary tangles, composed of hyper-phosphorylated forms of the microtubule-associated protein tau and extracellular senile plaques, composed

* Corresponding author. Tel.: +39 051 2099710; fax: +39 051 2099734.

E-mail address: angela.rampa@unibo.it (A. Rampa).

¹ Present address: Max-Planck-Institut für Molekulare Physiologie, Abteilung Chemische Biologie, Otto-Hahn-Str. 11, 44227 Dortmund, Germany.

of beta amyloid protein ($A\beta$) [3]. Although the steps connecting $A\beta$ to tau remain undefined, a growing body of genetic and biochemical evidence suggests that abnormal accumulation of $A\beta$ could trigger tau pathology, therefore placing amyloid aggregates upstream of neurofibrillary tangles and giving the former a central role in initiating the pathological cascade (amyloid hypothesis) [4].

Of considerable interest is also the role played by butyrylcholinesterase (BuChE), the second member of the cholinesterases family. In fact BuChE seems to be involved in the hydrolysis of ACh during the late stages of the disease (in compensation for the reduced levels of AChE) contributing to the breakdown of the neurotransmitter. Moreover, BuChE has been found to be responsible for up-regulating the expression of the amyloid precursor protein (APP) in cell membranes. Thereby, inhibition of BuChE could be regarded as an additional approach for the treatment of moderate forms of AD as it would result in the increase of ACh synaptic levels and the decrease of neurotoxic $A\beta$ fibrils [5,6].

Recently, the endocannabinoid system has attracted much interest as a novel therapeutic target involved in AD and other neurodegenerative diseases, due to potentially neuroprotective, anti-inflammatory and neurotrophic effect of certain cannabinoids. In particular, compounds that activate cannabinoid receptors of type 2 (CB2), either directly or by inhibiting endocannabinoid cellular reuptake or endocannabinoid inactivation by hydrolytic enzymes, have been suggested to produce beneficial effects in terms of both anti-inflammatory and neuroprotective effects and, subsequently, of anti-amnesic actions [7,8]. On the other hand, activation of cannabinoid receptors of type 1 (CB1) was suggested to either contribute to the amnesic actions of $A\beta$ or to counteract these actions, depending on the timing of the administration, and to inhibit $A\beta$ toxicity *in vitro*. These observations prompt the further testing of both CB1 agonists and antagonists and CB2 agonists, as

well as, under certain conditions, of inhibitors of endocannabinoid inactivation, for the treatment of $A\beta$ -induced toxicity and AD [7,8].

In the awareness of AD's multifaceted nature, one of the most promising therapeutic strategies to tackle this disorder is now based on the multi-target-directed ligand (MTDL) approach [9,10]. In line with this paradigm, in a previous communication, we reported the design, synthesis and biological evaluation of a small series of 2-arylbenzofurans of hybrid molecules [11]. From this collection, compound **1** (Fig. 1) emerged as a promising multi-target-directed lead, displaying anticholinesterase activity and $A\beta$ anti-aggregation properties, along with an additional neuroprotective effect in living human neuronal SH-SY5Y cells [11]. The benzofuran heterocyclic framework is now considered as a privileged structure, which is a common moiety found in many biologically active natural and therapeutic products and thus represents a very important pharmacophore. In particular, this scaffold is present in LY320135 (Fig. 1), a high affinity antagonist/inverse agonist at CB1 receptor [12]. Therefore, as a follow-up to our previous study, here we present the design, synthesis and biological evaluation of an extended collection of 2-arylbenzofuran derivatives, focused on the structure of **1**. Aimed at optimizing/improving the biological activities, and further exploring the chemical space of the selected targets, some modifications of the lead **1** were performed as reported in Fig. 1. The spacer between the 2-arylbenzofuran and the *N*-methyl-*N*-benzylamine moieties was varied to determine its optimal length, and the substituent in 3 position of the benzofuran scaffold was changed. Moreover, the *N*-methyl-*N*-benzylamine heptyloxy side chain was moved from the *para* to the *meta* position. In summary, a small library of 23 new derivatives was synthesized, whose structures are collected in Table 1. All compounds were tested for their biological activities towards selected targets involved in AD, namely human AChE and

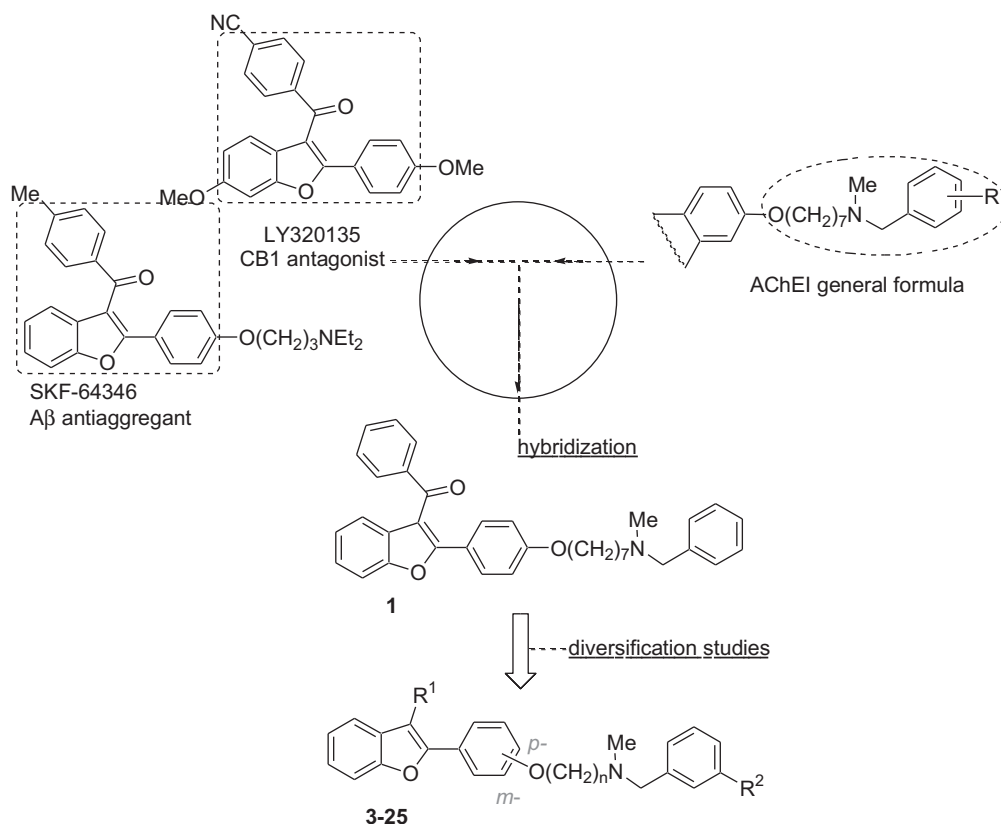


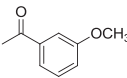
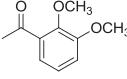
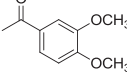
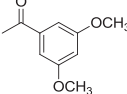
Fig. 1. Design of the studied compounds.

Table 1
Inhibitory activities on human AChE and BuChE expressed as IC₅₀ values of the studied compounds.

Comp.	R ¹	R ²	N	Chain	hAChE IC ₅₀ μM	BuChE IC ₅₀ μM	hBChE IC ₅₀ μM
1 ^a		H	7	<i>para</i>	40.7 ± 3.5		38.1 ± 2.2
2 ^a	H	H	7	<i>para</i>	32.6 ± 11.9		0.28 ± 0.02
3	H	H	3	<i>para</i>	n.a. ^b		136 ± 5
4	H	H	5	<i>para</i>	215 ± 1		6.60 ± 0.23
5	H	H	8	<i>para</i>	n.a. ^b		7.47 ± 0.34
6	H	H	9	<i>para</i>	n.a. ^b		55.6 ± 7.4
7	H	H	7	<i>meta</i>	n.a. ^b		3.00 ± 0.17
8		H	7	<i>para</i>	101 ± 21		60.1 ± 6.3
9		H	7	<i>para</i>	n.a. ^b		89.1 ± 9.9
10		H	7	<i>para</i>	n.a. ^b		88.9 ± 14.3
11		H	7	<i>para</i>	67.7 ± 1.3		81.2 ± 0.9
12		H	7	<i>para</i>	53 ± 10		3.18 ± 0.46
13		H	7	<i>para</i>	100 ± 18		9.42 ± 1.32
14		H	7	<i>para</i>	37.1 ± 6.0		1.81 ± 0.08
15		H	7	<i>para</i>	78 ± 21		23.0 ± 2.6
16		H	7	<i>para</i>	39.0 ± 0.5		21.0 ± 2.8
17		OCONHCH ₃	7	<i>para</i>	0.34 ± 0.03		0.88 ± 0.10
18		H	7	<i>meta</i>	0.24 ± 0.02		2.88 ± 0.26
19		H	7	<i>meta</i>	102 ± 18		0.40 ± 0.07
20		H	7	<i>meta</i>	n.a. ^b		43.9 ± 5.31

(continued on next page)

Table 1 (continued)

Comp.	R ¹	R ²	N	Chain	hAChE IC ₅₀ μM	BuChE IC ₅₀ μM
21		H	7	meta	n.a. ^b	1.97 ± 0.28
22		H	7	meta	n.a. ^b	1.37 ± 0.57
23		H	7	meta	n.a. ^b	3.01 ± 0.47
24		H	7	meta	n.a. ^b	2.51 ± 0.42
25		H	7	meta	n.a. ^b	0.048 ± 0.008
Rivastigmine ^c					3.01 ± 0.21	0.30 ± 0.01
Tacrine ^c					0.42 ± 0.02	0.046 ± 0.003
Galantamine ^c					2.01 ± 0.15	20.7 ± 1.5

Human recombinant AChE and BuChE from human serum were used. IC₅₀ values represent the concentration of inhibitor required to decrease enzyme activity by 50% and are the mean of two/three independent measurements, each performed in triplicate.

^a From ref. [11].

^b n.a. = not active. Compounds defined “not active” did not show any inhibitory activity when tested at a concentration equal to their maximum solubility in the assay conditions.

^c From ref. [37].

human BuChE, and Aβ fibril formation. On the basis of the results, some selected compounds were also tested for their ability to inhibit Aβ neurotoxicity in terms of neuronal viability loss, and to prevent Aβ peptide-binding to cell membrane and intracellular ROS formation in human neuronal SH-SY5Y cells.

Moreover, taking advantage of the presence of the benzofuran scaffold, we decided to evaluate the feasibility of extending the biological profile of the new compounds, merging in a single molecule potential activity at CB receptors as well. To this aim we tested all compounds for their affinity for CB1 and CB2 receptors.

2. Chemistry

The synthesis of the studied compounds was accomplished as shown in Scheme 1. Previously described benzofuran-based phenols [11,13] were *O*-alkylated by treatment with selected dihaloalkanes to afford the corresponding halo-alkoxy-derivatives **26–31**. Condensation with *N*-benzyl-*N*-methylamine in refluxing toluene afforded derivatives **3–7**. Next, a selection of acylchlorides was used for the tin(IV) chloride-promoted Friedel–Crafts acylation of the benzofuran scaffold, which occurred as expected only at position 3 of the heterocycle. Unfortunately, the resulting acyl derivatives **12–16** could be obtained only in poor yields (8–21%), most likely because the high affinity of the Lewis acid for the amino group in the side chain of **3–7** prevented its regeneration. To overcome this problem we performed the critical Friedel–Crafts acylation step prior to the condensation with *N*-benzyl-*N*-methylamine, although to the cost of a premature divergent step, requiring more purification efforts. Therefore, intermediates **28** and **31** were first converted into the 3-acyl-derivatives **32–44**, then treated with *N*-benzyl-*N*-methylamine to afford the desired products **8–11**, and **18–25**. Condensation of **36**

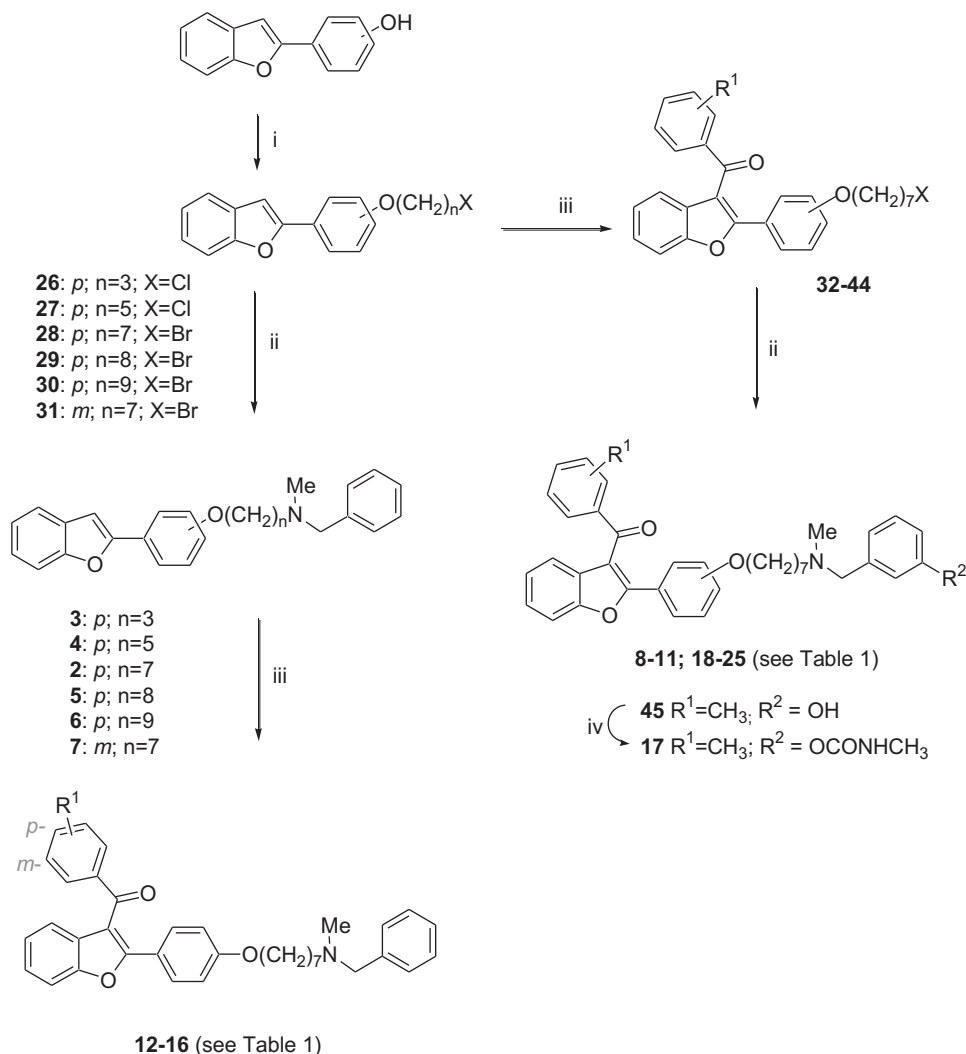
with 3-methylaminomethylphenol afforded **45** subsequently transformed into the *N*-methylcarbamate derivative **17**, by treatment with methyl isocyanate.

3. Biological evaluation

The inhibitory activities against both cholinesterases of the newly synthesized compounds were studied using the method described by Ellman [14] to determine the rate of acetylthiocholine or butyrylthiocholine hydrolysis in the presence of the inhibitor.

The inhibition of Aβ fibril formation was studied with an *in vitro* assay that uses UV–vis measurements [15]. In this assay the Aβ_{25–35} peptide, which preserves the properties of neurotoxicity and aggregation, was used [16,17]. For the compounds exhibiting an inhibitory activity at least equal to that of curcumin (as reference compound endowed with antiamyloidogenic properties [18]), IC₅₀ values were calculated. The neuroprotective effects of the most interesting Aβ antiaggregating compounds against the Aβ_{25–35} peptide induced toxicity in human neuronal SH-SY5Y cells were also determined using a colorimetric MTT assay [19]. In parallel, the ability of the same compounds to inhibit Aβ_{25–35} peptide-binding to cell membrane and Aβ_{25–35} peptide-induced ROS formation was investigated using Congo Red (CR) and DHE assay, respectively [20].

Finally, the effect of the new compounds on [³H]-CP55940 binding to human recombinant cannabinoid CB1 and CB2 receptors was analysed. The activities, expressed as IC₅₀, were determined by non-linear regression of the inhibition of radioligand binding exerted by increasing concentrations of test compounds. When the IC₅₀ value was lower than 10 μM, the *K_i* value was calculated by applying the Cheng–Prusoff equation to the IC₅₀ value.



Reagents and conditions: i) $\text{Br}(\text{CH}_2)_n\text{X}$, K_2CO_3 , acetone, reflux, 24 h; ii) *N*-methyl-*N*-benzylamine or *N*-(3-hydroxybenzyl)methylamine, toluene, reflux; iii) selected acylchloride, SnCl_4 , DCM, r.t.; iv) CH_3NCO , NaH, rt, 24 h.

Scheme 1. Synthesis of the studied compounds.

4. Results and discussion

The inhibitory activities against both recombinant human AChE (hAChE) and BuChE from human serum (hBuChE) of new derivatives, together with those of the lead compound **1**, and the reference compounds rivastigmine, tacrine and galantamine, are reported in Table 1, and are expressed as IC_{50} values.

To assess the importance of the heptyloxy chain spacer of the lead **1**, its length was varied, to obtain compounds **3–6**, where $n = 3, 5, 8, 9$. All compounds proved to be almost inactive on hAChE, and remarkably less active toward hBuChE than the reference compound **2** (not acylated precursor of **1**, bearing a heptyloxy spacer [11]). Then, once the best chain length was established, different acyl groups were inserted in position 3 of the benzofuran scaffold of compound **2**, to explore the chemical space on the different targets. Compounds **8–11**, bearing bulky and lipophilic groups, showed lower activity than the lead compound **1** on both hAChE and hBuChE. Compounds **12–16**, carrying an additional amino moiety, did not show an improvement of AChE inhibition, still keeping a fairly good BuChE inhibition.

Moving the heptyloxy chain of **2** from the *para* to the *meta* position of the phenyl ring (compound **7**) lowered the activity toward hBuChE and abolished hAChE inhibition. Nevertheless, compound **7** was acylated with the groups that proved to be favourable for activity in the *para* series, to obtain compounds **18–25**. Interestingly, compound **18**, bearing the same unsubstituted benzoyl group of **1**, was the most active of the series on hAChE inhibition, showing a sub-micromolar IC_{50} value, thus being 180 fold more potent than **1**. The insertion of substituents on the benzoyl moiety (compounds **19–25**) led to almost inactive derivatives on this target. Conversely, compounds **19** (with a 2-methylbenzoyl group) and **25** (with a 2,4 dimethoxybenzoyl substituent) emerged for their remarkable activity on hBuChE, being **25** the most active ($\text{IC}_{50} = 48 \text{ nM}$) of the series and highly selective. Finally, compound **17** bearing a methylcarbamic group (acting as a pseudo-irreversible inhibitor, as already reported in previous papers for carbamate analogues [21,22]), showed an improvement of potency of one order of magnitude on hAChE and retained a very good activity toward hBuChE, when compared to the marketed drug rivastigmine.

The benefit of having cholinesterase inhibitors able of modulating the brain activity of a single enzyme in a highly selective manner or both cholinesterases has been debated since non-cholinergic activities of AChE and the cholinergic role of BuChE over AD progression were discovered. Indeed, AChE is principally associated with neurons and axons, while BuChE is primarily expressed and secreted by glial cells within the brain [23]. In the healthy human brain, AChE and BuChE are found in the ratio of 4:1. However, in the brains of AD patients AChE activity can decline by up to 45% during disease progression, reflecting the disappearance of neurons and axons to which it is associated, while BuChE activity can be elevated by up to 2-fold [5], thereby considerably altering this ratio. Furthermore, the dual AChE/BuChE inhibitor rivastigmine demonstrated beneficial effects on memory acquisition and consolidation. This may involve direct classical cholinergic augmentation, together with a cholinergically-mediated protective action, potentially *via* the reduction of inflammation [24]. Therefore, a comparable profile could also be envisaged for the dual AChE/BuChE inhibitor **17** and for the BuChE selective derivatives **19** and **25**.

Regarding $A\beta$ fibril inhibition, the chain length turned out to play an important role, since the propyloxy derivative **3** showed poor inhibition, while moving through the homologous series the activity rose. Pentyloxy (**4**) and octyloxy (**5**) derivatives showed the same activity as curcumin, while the nonyloxy derivative **6** was more active ($IC_{50} = 5.5 \mu M$). Regarding compounds **8–11**, with bulky and aromatic groups in 3 position of the benzofuran scaffold, only compound **8** retained the activity of the lead compound **1**, while **11** surprisingly showed a proaggregatory activity (Fig. 2).

Compounds **12–16**, carrying an additional amino moiety, proved to weakly inhibit amyloid aggregation. The most potent inhibitor of the series was **7**, obtained by moving the heptyloxy chain to the *meta* position (Fig. 3), 2.5 times more active when compared to curcumin ($IC_{50} = 3.9$ and $10 \mu M$, respectively). In the *meta* series, **18** and **19** retained the activity of the lead compound **1**. For compounds exhibiting an inhibitory activity at least equal to that of curcumin, IC_{50} values were calculated as reported in Table 2.

Aggregation of monomeric $A\beta$ species into higher molecular weight oligomers produces the primary neurotoxic species in AD [25]. Indeed, oligomer species of aggregated $A\beta$ exert toxic effects on synaptic and cellular functions [26], finally leading to neurodegeneration and cognitive, as well as neuropsychiatric, symptoms. Thus, compounds that are able to slow down or block the amyloid polymerization process could be considered potential drugs for inhibition of AD progression [27].

The neuroprotective effects of the most interesting $A\beta$ anti-aggregating compounds (**7**, **8**, **18**, **19**) were determined against the $A\beta_{25-35}$ peptide induced toxicity in human neuronal SH-SY5Y cells. Compounds **18** and **19**, but not **7** and **8**, showed a similar neuroprotective effect against $A\beta_{25-35}$ peptide induced neurotoxicity (Table 2). As reported in Fig. 4, treatment of SH-SY5Y cells with both

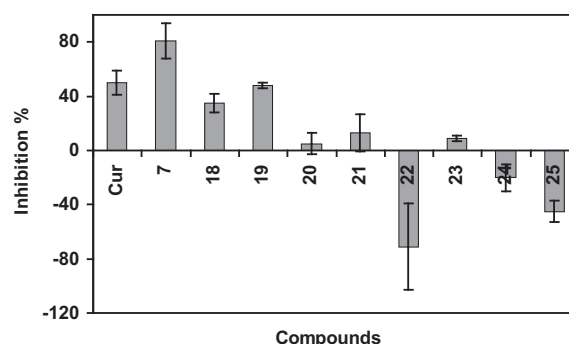


Fig. 3. $A\beta_{25-35}$ fibril inhibition by *meta* substituted compounds compared to that of curcumin (Cur). Means and SD of three independent experiments are shown.

compounds **18** and **19** at 10 and $30 \mu M$ significantly reduced the neuronal viability loss evoked by $A\beta_{25-35}$ peptide, in a dose-dependent manner. Since the same trend was observed with compound **1**, these results proved that moving the heptyloxy chain from the *para* to the *meta* position of the phenyl ring did not influence the observed neuroprotective effects. Therefore, the benzoyl group of compound **1** (maintained also in **18**, and with a little change in **19**) is crucial for the interaction with hydrophobic residues of $A\beta_{25-35}$ peptide, such as Ile31, Ile32 and Met35, that are critical for both neurotoxicity and aggregation processes [17,28]. The lack of neuroprotective effect shown in this cellular assay by **7**, that proved to be the most potent antiaggregating compound in the *in vitro* assay, could probably be ascribed to its lower $\log P$ (6.80) with respect to **1** ($\log P = 8.00$), **18** ($\log P = 8.00$) and **19** ($\log P = 8.49$), as already pointed out in a previous paper [11].

In this context, recent studies have suggested that unaggregated $A\beta_{25-35}$ and $A\beta_{31-35}$ peptides could initiate a cascade of events leading to neurotoxicity solely after their internalization within the neuronal cells [29]. These findings prompted us to evaluate the ability of compounds **1**, **18** and **19** to prevent the binding between the $A\beta_{25-35}$ peptide and the plasma membrane surface. The binding of $A\beta_{25-35}$ peptide ($10 \mu M$) with SH-SY5Y cells reached a maximum in 30 min and was significantly reduced by co-treatment with compounds **1**, **18** and **19** ($30 \mu M$), as determined by the CR assay (Fig. 5). In parallel, the oxidative stress in SH-SY5Y cells, in terms of intracellular ROS formation evoked by $A\beta_{25-35}$ peptide ($10 \mu M$) was also investigated. Recent studies show that ROS formation is directly related to membrane perturbation by

Table 2

$A\beta$ fibril formation inhibitory activity and effects of selected compounds on $A\beta_{25-35}$ peptide induced neurotoxicity in SH-SY5Y cells.

Compound	$A\beta_{25-35}$ fibril inhibition (%) ^a	$A\beta_{25-35}$ $IC_{50} \mu M$ ^b	SH-SY5Y cells PI ^c
1	47	12.5	58.16 ± 3.45
7	81	3.9	n.d.
8	48	—	n.d.
18	35	—	48.35 ± 4.68
19	48	—	46.20 ± 5.40

n.d. = PI not determined because protective effects were not observed at highest tested concentration.

^a see Figs. 2 and 3.

^b IC_{50} values defined as the concentrations of inhibitor to inhibit the formation of $A\beta_{25-35}$ fibrils to 50% of the control value (reference compound: curcumin $IC_{50} = 10.0 \mu M$).

^c Percentage Inhibition (PI) observed at highest tested concentration. The neuronal viability in SH-SY5Y cells was determined by MTT assay (as described in Experimental section), after 3 h of incubation with $A\beta_{25-35}$ peptide ($10 \mu M$) in the presence or absence of various compounds ($30 \mu M$). The values are the mean \pm SD of at least two independent experiments.

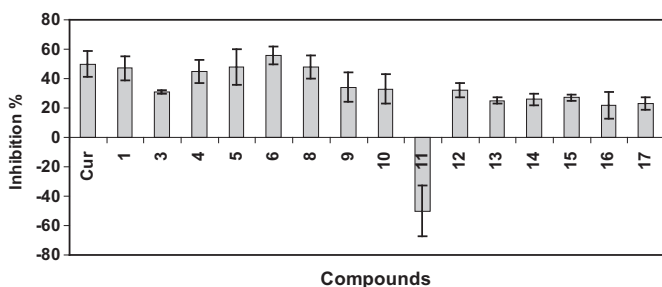


Fig. 2. $A\beta_{25-35}$ fibril inhibition by *para* substituted compounds compared to that of curcumin (Cur). Means and SD of three independent experiments are shown.

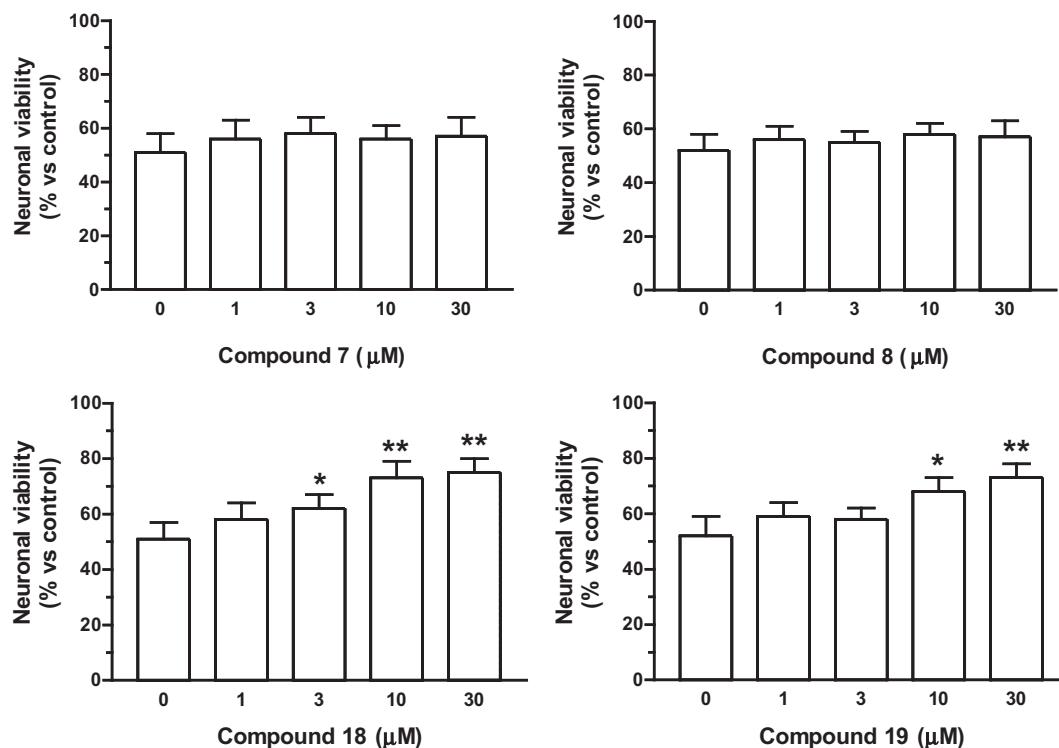


Fig. 4. Effects of selected compounds on $A\beta_{25-35}$ peptide-induced neurotoxicity in SH-SY5Y cells. The neuronal viability in SH-SY5Y cells was determined by MTT assay (as described in the Experimental section), after 3 h of incubation with $A\beta_{25-35}$ peptide (10 μM) in the presence or absence of various concentrations of compounds (1–30 μM). The values are reported as mean \pm SD of three independent experiments (* p < 0.05, ** p < 0.01, vs. untreated cells, ANOVA with Dunnett's test).

amyloid peptide [30,31]. Remarkably, compounds **1**, **18** and **19** (30 μM) significantly inhibited the $A\beta_{25-35}$ peptide-induced ROS formation (Fig. 6). Taken together, these results showed the ability of compound **1**, **18** and **19** to counteract the neurotoxicity of $A\beta_{25-35}$

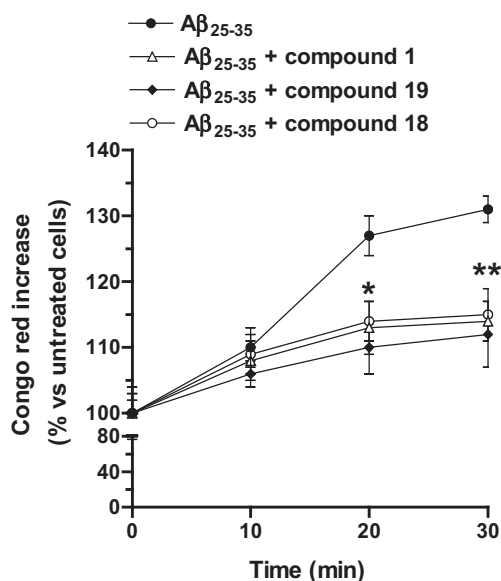


Fig. 5. Effects of selected compounds on the binding of $A\beta_{25-35}$ peptide with SH-SY5Y cells. SH-SY5Y cells were treated with $A\beta_{25-35}$ peptide (10 μM) for different time in the presence or absence of compounds **1**, **18** and **19** (30 μM). At the end of incubation, the $A\beta_{25-35}$ peptide binding to plasma membrane was determined by CR assay and the results are expressed as percentage of control cells (* p < 0.05, ** p < 0.01, vs. untreated cells with $A\beta_{25-35}$ peptide at Student's t -test).

peptides, suggesting their peculiar ability to prevent the interaction between $A\beta_{25-35}$ peptides and the cell membrane of SH-SY5Y cells, responsible for the ROS formation as well as neuronal viability loss.

Finally, with respect to the feasibility of merging in a single molecule different biological profiles, the new compounds were tested for their ability of targeting cannabinoid receptors (Table 3). As expected from their similarity to the heterocyclic pharmacophore present in LY320135, compound **1**, and to a lesser extent its precursor compound **2**, exhibited a good selectivity and a moderate affinity for human recombinant CB1 receptors. When replacing the phenyl ring in position 3 of **1** with bulkier acyl groups (compounds **8–11**), only compound **10**, bearing the biphenyl moiety, showed an appreciable, although unselective, affinity for CB2. Furthermore, the introduction of an amino moiety on the benzoyl group (compounds **12–16**), could improve the activity, depending on the type and the position of the substituent: the position (4 vs. 3) of the amine group appeared to modulate affinity and strongly increase selectivity for CB2 vs. CB1 (see **14** vs. **15** or **13**). On the contrary, the compounds of the *meta* series (**18–25**) were inactive (data not shown). These results prove the moving the heptyloxy chain from the *para* to the *meta* position is detrimental for activity.

Taking into account our aim of identifying new multi-target directed ligands, **18** emerged as a promising compound, since it proved to be remarkably more active than **1** on both AChE and BuChE, maintained good $A\beta$ antiaggregating properties and showed the best neuroprotective profile, being capable of restoring cell viability by 48%. Moreover, it also proved to be endowed with interesting effects in additional biological studies, since it was able to prevent the binding of the $A\beta_{25-35}$ peptide to the plasma membrane surface and to inhibit $A\beta_{25-35}$ peptide-induced ROS formation. Although it is generally expected for a multi-target ligand that the activities on the different targets would be appropriately balanced, the levels of these biological counterparts should

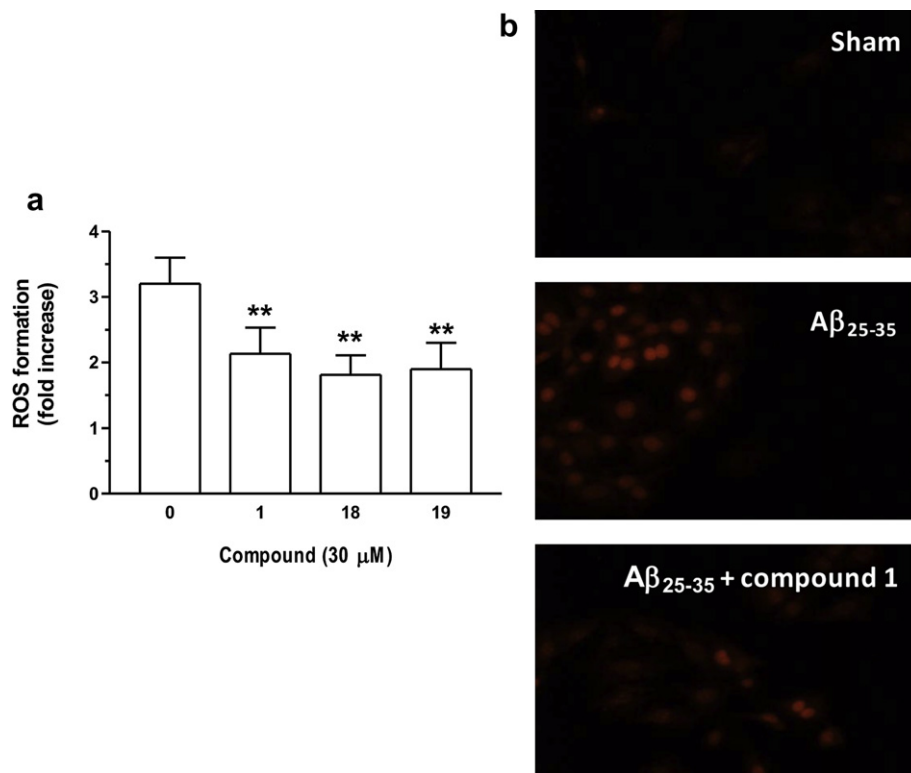


Fig. 6. Effects of selected compounds on $A\beta_{25-35}$ peptide-induced ROS formation in SH–SY5Y cells. (a) SH–SY5Y cells were treated with $A\beta_{25-35}$ peptide (10 μM) in the absence or presence of compounds **1**, **18** and **19** (30 μM) for 3 h. At the end of incubation, ROS formation was determined using a fluorescence probe, DHE, as described in the Experimental section. Four randomly selected areas with 50–100 cells in each were analysed under a fluorescence microscope and the values obtained are expressed as densitometry/cell. Values are shown as mean \pm SD of three independent experiments (** $p < 0.01$, vs. untreated cells at Student's t -test). (b) Representative images of ROS formation. Scale bars: 100 μm .

also be taken into account in order to appropriately evaluate its efficacy. Considering the levels of amyloid-peptide in the cerebrospinal fluid of patients afflicted with mild cognitive impairment or sporadic AD are in the sub-nanomolar range [32] new inhibitors might potentially exert their neuroprotective effects when a sub-nanomolar concentration is reached. Moreover, on the basis of the cholinesterase level in AD patients [33], it also seems plausible that compounds with anti-cholinesterase activity in the sub-micromolar range might simultaneously inhibit amyloid aggregation if a concentration close to their IC_{50} values is locally reached.

Noteworthy, the extension of the biological studies by exploitation of these new assays allowed us to broaden the profile of the lead compound **1**, which was also able to counteract the

neurotoxicity of $A\beta_{25-35}$ peptide by preventing the interaction between this peptide and the cell membrane of SH–SY5Y cells, responsible for ROS formation and neuronal viability loss. In addition, **1** showed good selectivity and moderate affinity for CB1 receptors. The higher cytoprotection activity of **1**, with respect to **18** and **19**, could thus be ascribed to its affinity for CB1 receptors, known to be expressed in SH–SY5Y cells [34,35]. In this regard, a recent study suggests that CB1 receptor activation exerts a strong neuroprotection action against $A\beta$ -induced neurotoxicity [36].

5. Conclusions

In continuing our studies on the design of new multi-target compounds for the treatment of AD, we performed several modifications of the promising hit **1**, previously identified among a new series of hybrid molecules based on the frameworks of our AChE/BuChE inhibitors and of SKF-64346 [11].

With the aim of further optimizing this scaffold and broadening the biological profile of the molecules by investigating their potential action on additional targets involved in AD, a small library of compounds was prepared. The different modifications introduced in the structure of the lead compound led to an increase in activity towards one or more of the selected targets, compounds **19** and **25** being potent BuChE inhibitors, carbamate **17** showing higher activity than the marketed drug rivastigmine on both AChE and BuChE and **7** inhibiting $A\beta$ fibril formation *in vitro* up to 81%, but failed to protect neuronal cells from $A\beta$ toxicity.

The most interesting multi-target compounds proved to be **18**, and **1**, being able to address all the selected targets. Noteworthy, **1** also showed good selectivity and moderate affinity for CB1 receptors, opening new perspectives in the field of research on AD.

Table 3

Effect of studied compounds on [^3H]-CP55940 binding to the human recombinant cannabinoid receptors. Percent of binding displacement at the maximum concentration tested is also reported.

Comp	EC_{50} on CB1 μM	K_i on CB1 μM	Max tested (% displacement)	EC_{50} on CB2 μM	K_i on CB2 μM	Max tested (% displacement)
1	0.79	0.32	10 μM (8.72%)	>10	>10	10 μM (47.32%)
2	6.95	2.80	10 μM (57.83%)	>10	>10	10 μM (21.78%)
8	>10	>10	10 μM (13.81%)	>10	>10	10 μM (8.90%)
9	>10	>10	10 μM (35.06%)	>10	>10	10 μM (6.87%)
10	7.74	3.12	25 μM (80.00%)	7.06	1.79	25 μM (86.00%)
11	>10	>10	10 μM (30.34%)	>10	>10	10 μM (9.87%)
12	>10	>10	10 μM (29.75%)	>10	>10	10 μM (47.27%)
13	>10	>10	10 μM (47.70%)	4.40	1.12	10 μM (65.17%)
14	6.38	2.57	10 μM (76.50%)	2.71	0.69	10 μM (77.91%)
15	>10	>10	10 μM (35.18%)	4.65	1.18	10 μM (92.00%)
16	1.37	0.55	10 μM (83.12%)	2.27	0.58	10 μM (70.58%)

Data are reported as means of at least $n = 3$ experiments. SEMs are not shown, but they were always less than 10% of the mean.

In conclusion, these studies indicate that it is possible to obtain compounds capable of modulating both classic and novel, emerging targets involved in AD. These new compounds could serve as a platform for further studies aimed at fine-tuning their multifaceted activities for the identification of new molecular entities endowed with broader biological profile in awareness of the emerging multi-target paradigm for drug discovery.

6. Experimental section

6.1. Chemistry. General methods

Melting points were measured in glass capillary tubes on a Büchi SMP-20 apparatus and are uncorrected. Direct infusion ES-MS spectra were recorded on a Waters Micromass ZQ 4000 apparatus. ¹H NMR spectra were recorded in CDCl₃ solution on a Varian Gemini 300/400 MHz spectrometer. Chemical shifts are reported in parts per million (ppm) relative to tetramethylsilane (TMS), and spin multiplicities are given as s (singlet), d (doublet), t (triplet), m (multiplet) or br (broad). Chromatographic separations were performed on silica gel columns (Kieselgel 40, 0.040–0.063 mm; Merck) by flash chromatography. Analyses indicated by the symbols of the elements were within ±0.4% of the theoretical values. Compounds were named following IUPAC rules as applied by Beilstein-Institut AutoNom (version 2.1), a PC integrated software package for systematic names in organic chemistry.

6.1.1. 2-[4-(3-Chloropropoxy)phenyl]benzofuran (26)

A stirred mixture of 4-benzofuran-2-yl-phenol [11] (1 g, 4.7 mmol), 1-bromo-3-chloropropane (0.94 mL, 9.5 mmol) and K₂CO₃ (1.2 g) was refluxed in acetone (100 mL) for 20 h. The suspension was filtered while hot and the solvent was removed under reduced pressure. After adding petroleum ether, the residue was kept in the freezer overnight and the white solid that formed was filtered off, affording **26** (0.93 g, 69%). mp 137–138 °C. ¹H NMR δ: 2.23–2.31 (m, 2H), 3.77–3.80 (m, 2H), 4.20 (t, *J* = 6.0 Hz, 2H), 6.87 (s, 1H), 6.96 (d, *J* = 8.3 Hz, 2H), 7.18–7.32 (m, 2H), 7.47–7.58 (m, 2H), 7.78 (d, *J* = 8.4, 2H).

6.1.2. 2-[4-(5-Chloropentyloxy)phenyl]benzofuran (27)

Using the previous procedure and starting from 4-benzofuran-2-yl-phenol [11] (0.34 g, 1.6 mmol) and 1-bromo-5-chloropentane (0.42 mL, 3.2 mmol), **27** (0.35 g, 69%) was obtained as a white solid. mp 115 °C. ¹H NMR δ: 1.60–1.71 (m, 2H), 1.83–1.90 (m, 4H), 3.58 (t, *J* = 6.3 Hz, 2H), 4.03 (t, *J* = 6.0 Hz, 2H), 6.88 (s, 1H), 6.96 (d, *J* = 8.4 Hz, 2H), 7.21–7.26 (m, 2H), 7.48–7.56 (m, 2H), 7.76 (d, *J* = 8.4, 2H).

6.1.3. 2-[4-(7-Bromoheptyloxy)phenyl]benzofuran (28)

Using the previous procedure and starting from 4-benzofuran-2-yl-phenol [11] (0.35 g, 1.6 mmol) and 1,7-dibromoheptane (0.57 mL, 3.3 mmol), **28** (0.34 g, 58%) was obtained as a white solid. mp 92 °C. ¹H NMR δ: 1.25–1.60 (m, 6H), 1.71–1.98 (m, 4H), 3.42 (t, *J* = 5.0 Hz, 2H), 4.01 (t, *J* = 6.0 Hz, 2H), 6.87 (s, 1H), 6.91 (d, *J* = 8.4 Hz, 2H), 7.23–7.29 (m, 2H), 7.49–7.58 (m, 2H), 7.76 (d, *J* = 8.4 Hz, 2H).

6.1.4. 2-[4-(8-Bromooctyloxy)phenyl]benzofuran (29)

Using the previous procedure and starting from 4-benzofuran-2-yl-phenol [11] (0.45 g, 2.1 mmol) and 1,8-dibromooctane (0.79 mL, 4.3 mmol), **29** (0.51 g, 61%) was obtained as a white solid. mp 112 °C. ¹H NMR δ: 1.37–1.58 (m, 8H), 1.76–1.92 (m, 4H), 3.42 (t, *J* = 6.0 Hz, 2H), 4.00 (t, *J* = 6.6 Hz, 2H), 6.88 (s, 1H), 6.96 (d, *J* = 8.0 Hz, 2H), 7.20–7.25 (m, 2H), 7.48–7.56 (m, 2H), 7.75 (dd, *J*₁ = 2.1 Hz; *J*₂ = 8.4 Hz, 2H).

6.1.5. 2-[4-(9-Bromononyloxy)phenyl]benzofuran (30)

Using the previous procedure and starting from 4-benzofuran-2-yl-phenol [11] (0.57 g, 2.7 mmol) and 1,9-dibromononane (1.1 mL, 5.4 mmol), **30** (0.82 g, 73%) was obtained as a white solid. mp 108 °C. ¹H NMR δ: 1.34–1.56 (m, 10H), 1.76–1.95 (m, 4H), 3.41 (t, *J* = 6.0 Hz, 2H), 4.00 (t, *J* = 6.6 Hz, 2H), 6.88 (s, 1H), 6.96 (d, *J* = 8.3 Hz, 2H), 7.20–7.25 (m, 2H), 7.48–7.56 (m, 2H), 7.75 (dd, *J*₁ = 2.1 Hz; *J*₂ = 6.9 Hz, 2H).

6.1.6. 2-[3-(7-Bromoheptyloxy)phenyl]benzofuran (31)

Using the previous procedure and starting from 3-benzofuran-2-yl-phenol [13] (2.65 g, 13 mmol) and 1,7-dibromoheptane (4.3 mL, 25 mmol), **31** (4 g, 81%) was obtained as a white solid. mp 145 °C. ¹H NMR δ: 1.23–1.58 (m, 6H), 1.69–1.98 (m, 4H), 3.37–3.42 (m, 2H), 4.01 (t, *J* = 6.4 Hz, 2H), 6.89 (s, 1H), 6.93 (d, *J* = 8.4 Hz, 2H), 7.24–7.31 (m, 2H), 7.50–7.56 (m, 2H), 7.79 (d, *J* = 8.4, 2H).

6.1.7. [3-(4-Benzofuran-2-yl-phenoxy)propyl]benzylmethylamine (3)

A stirred solution of **26** (0.9 g, 3.1 mmol) and *N*-benzyl-*N*-methylamine (0.80 mL, 6.2 mmol) in toluene (100 mL) was refluxed in the presence of a catalytic amount of NaI for 20 h. The mixture was washed with water (3 × 25 mL) and the organic layer was dried over Na₂SO₄. The solvent was removed under reduced pressure and the residue was purified by flash chromatography on silica gel (toluene/acetone 96:4), affording **3** as a yellowish solid (1.1 g, 95%). mp 84 °C. ¹H NMR δ: 1.96–2.04 (m, 2H), 2.23 (s, 3H), 2.52–2.60 (m, 2H), 3.51 (s, 2H), 4.09 (t, *J* = 6.6 Hz, 2H), 6.86 (s, 1H), 6.96 (d, *J* = 8.0 Hz, 2H), 7.15–7.30 (m, 7H), 7.45–7.55 (m, 2H), 7.75–7.80 (m, 2H). ES-MS *m/z*: 372 (M + 1). Anal. C₂₅H₂₅NO₂ (C, H, N).

6.1.8. [5-(4-Benzofuran-2-yl-phenoxy)pentyl]benzylmethylamine (4)

Using the previous procedure and starting from **27** (0.34 g, 1.6 mmol), **4** was obtained as a yellowish solid (0.26 g, 40%). mp 57 °C. ¹H NMR δ: 1.47–1.59 (m, 4H), 1.75–1.81 (m, 2H), 2.18 (s, 3H), 2.34–2.41 (m, 2H), 3.47 (s, 2H), 3.92–3.99 (t, *J* = 6.2 Hz, 2H), 6.84 (s, 1H), 6.90–6.95 (d, *J* = 8.8 Hz, 2H), 7.18–7.31 (m, 7H), 7.46–7.51 (m, 2H), 7.73–7.78 (d, *J* = 8.8 Hz, 2H). ES-MS *m/z*: 400 (M + 1). Anal. C₂₇H₂₉NO₂ (C, H, N).

6.1.9. [8-(4-Benzofuran-2-yl-phenoxy)octyl]benzylmethylamine (5)

Using the previous procedure and starting from **29** (0.51 g, 1.3 mmol), **5** was obtained as a white solid (0.2 g, 36%). mp 69–70 °C. ¹H NMR δ: 1.32–1.58 (m, 10H), 1.75–1.85 (m, 2H), 2.18 (s, 3H), 2.32–2.39 (m, 2H), 3.47 (s, 2H), 4.00 (t, *J* = 6.2 Hz, 2H), 6.84 (s, 1H), 6.96 (d, *J* = 8.8 Hz, 2H), 7.19–7.32 (m, 7H), 7.47–7.54 (m, 2H), 7.78 (d, *J* = 8.8 Hz, 2H). ES-MS *m/z*: 442 (M + 1). Anal. C₃₀H₃₅NO₂ (C, H, N).

6.1.10. [9-(4-Benzofuran-2-yl-phenoxy)nonyl]benzylmethylamine (6)

Using the previous procedure and starting from **30** (0.82 g, 2.0 mmol), **6** was obtained as a white solid (0.53 g, 58%). mp 79 °C. ¹H NMR δ: 1.34–1.53 (m, 12H), 1.75–1.86 (m, 2H), 2.22 (s, 3H), 2.37–2.42 (m, 2H), 3.51 (s, 2H), 4.04 (t, *J* = 6.6 Hz, 2H), 6.91 (s, 1H), 6.97 (d, *J* = 8.8 Hz, 2H), 7.24–7.36 (m, 7H), 7.52–7.58 (m, 2H), 7.82 (dd, *J*₁ = 2.0 Hz; *J*₂ = 8.0 Hz, 2H). ES-MS *m/z*: 456 (M + 1). Anal. C₃₁H₃₇NO₂ (C, H, N).

6.1.11. [7-(3-Benzofuran-2-yl-phenoxy)heptyl]benzylmethylamine (7)

Using the previous procedure and starting from **31** (4 g, 10 mmol), **7** was obtained as a yellowish oil (0.84 g, 20%). ¹H NMR δ: 1.20–1.59 (m, 8H), 1.69–1.87 (m, 2H), 2.17 (s, 3H), 2.32–2.39 (m, 2H), 3.42 (s, 2H), 3.97 (t, *J* = 6.2 Hz, 2H), 6.84 (s, 1H), 6.93 (d, *J* = 8.8 Hz, 2H), 7.18–7.31 (m, 7H), 7.46–7.51 (m, 2H), 7.75 (d, *J* = 8.8 Hz, 2H). ES-MS *m/z*: 428 (M + 1). Anal. C₂₉H₃₃NO₂ (C, H, N).

6.1.12. (2-{4-[7-(Benzylmethylamino)heptyloxy]phenyl}benzofuran-3-yl)-[3-(diethylaminomethyl)-phenyl]methanone (**12**)

To a cooled solution (0 °C) of **2** [11] (0.43 g, 1.0 mmol) and 3-chloromethylbenzoyl chloride (0.24 g, 1.25 mmol) in dry CH₂Cl₂ (50 mL), SnCl₄ (0.32 g, 1.25 mmol) was added dropwise with stirring. The mixture was allowed to reach room temperature then stirred overnight. The reaction was quenched with ice/water and stirred for 30 min. The organic layer was washed with water (3 × 10 mL) and with brine (3 × 10 mL), then dried over Na₂SO₄ and the solvent was removed under reduced pressure. The crude was purified by flash chromatography (toluene/acetone 60:40), affording (2-{4-[7-(benzylmethylamino)heptyloxy]phenyl}benzofuran-3-yl)-[3-(2-chloroethoxy)phenyl]methanone as a dark yellow oil (0.26 g, 43%). ¹H NMR δ: 1.02–1.60 (m, 8H), 1.62–1.88 (m, 2H), 2.20 (s, 3H), 2.33–2.44 (m, 2H), 3.46 (s, 2H), 3.91 (t, J = 6.4 Hz, 2H), 4.58 (s, 2H), 6.80 (d, J = 8.4 Hz, 2H), 7.05–7.38 (m, 11H), 7.50–7.63 (m, 4H), 7.79–7.92 (m, 2H). A stirred solution of this compound (0.26 g, 0.45 mmol) and diethylamine (0.1 mL, 0.90 mmol) was refluxed in toluene (100 mL) for 20 h in the presence of NaI. The mixture was washed with water (3 × 25 mL), then with brine (3 × 25 mL). The organic layer was collected and dried over Na₂SO₄. The solvent was removed under reduced pressure and the residue was purified by flash chromatography (toluene/acetone 60:40), affording **12** as a yellow oil (0.05 g, 18%). ¹H NMR δ: 1.01 (t, J = 6.4 Hz, 6H), 1.22–1.58 (m, 8H), 1.62–1.82 (m, 2H), 2.20 (s, 3H), 2.35–2.46 (m, 6H), 3.45 (s, 2H), 3.58 (s, 2H), 3.89 (t, J = 6.6 Hz, 2H), 6.81 (d, J = 8.4 Hz, 2H), 7.10–7.38 (m, 10H), 7.49–7.61 (m, 4H), 7.81–7.93 (m, 2H). ES-MS *m/z*: 617 (M + 1). Anal. C₄₁H₄₈N₂O₃ (C, H, N).

6.1.13. (2-{4-[7-(Benzylmethylamino)heptyloxy]phenyl}benzofuran-3-yl)-[4-(diethylaminomethyl)-phenyl]methanone (**13**)

Using the same procedure and starting from **2** [11] (0.43 g, 1.0 mmol) and 4-chloromethylbenzoyl chloride (0.24 g, 1.25 mmol), (2-{4-[7-(benzylmethylamino)heptyloxy]phenyl}benzofuran-3-yl)-[4-(2-chloroethoxy)phenyl]methanone was obtained after flash chromatography (toluene/acetone 60:40), as a dark yellow oil (0.27 g, 45%). ¹H NMR δ: 1.00–1.58 (m, 8H), 1.64–1.90 (m, 2H), 2.19 (s, 3H), 2.35–2.46 (m, 2H), 3.45 (s, 2H), 3.86 (t, J = 6.8 Hz, 2H), 4.59 (s, 2H), 6.79 (d, J = 8.4 Hz, 2H), 7.05–7.38 (m, 11H), 7.49–7.61 (m, 4H), 7.81–7.93 (m, 2H). A stirred solution of this compound (0.26 g, 0.45 mmol) and diethylamine (0.1 mL, 0.90 mmol) was refluxed in toluene (100 mL) for 20 h in the presence of a catalytic amount of NaI. The mixture was washed with water (3 × 25 mL), then with brine (3 × 25 mL). The organic layer was collected and dried over Na₂SO₄. The solvent was removed and the residue was purified by flash chromatography (toluene/acetone 60:40), affording **13** as a yellow oil (0.05 g, 18%). ¹H NMR δ: 1.01 (t, J = 6.4 Hz, 6H), 1.22–1.58 (m, 8H), 1.62–1.82 (m, 2H), 2.20 (s, 3H), 2.35–2.46 (m, 6H), 3.45 (s, 2H), 3.58 (s, 2H), 3.89 (t, J = 6.4 Hz, 2H), 6.81 (d, J = 8.4 Hz, 2H), 7.10–7.38 (m, 10H), 7.49–7.61 (m, 4H), 7.81–7.93 (m, 2H). ES-MS *m/z*: 617 (M + 1). Anal. C₄₁H₄₈N₂O₃ (C, H, N).

6.1.14. (2-{4-[7-(Benzylmethylamino)heptyloxy]phenyl}benzofuran-3-yl)-[3-(2-diethylaminoethoxy)phenyl]methanone (**14**)

To a cooled solution (0 °C) of **2** [11] (1.2 g, 2.8 mmol) and 3-(2-chloroethoxy)benzoyl chloride (0.73 g, 3.4 mmol) in dry CH₂Cl₂ (50 mL), SnCl₄ (0.87 g, 3.4 mmol) was added dropwise with stirring. The mixture was allowed to reach room temperature then stirred overnight. The reaction was quenched with ice/water and stirred for 30 min. The organic layer was washed with water (3 × 10 mL) and brine (3 × 10 mL), then dried over Na₂SO₄ and the solvent was removed. The crude was purified by flash chromatography (toluene/acetone 20:80), affording (2-{4-[7-(benzylmethylamino)heptyloxy]phenyl}benzofuran-3-yl)-[4-(2-chloroethoxy)phenyl]methanone as a dark yellow oil (0.92 g, 54%). ¹H NMR δ: 1.17–1.59

(m, 8H), 1.60–1.85 (m, 2H), 2.19 (s, 3H), 2.30–2.37 (t, 2H), 3.45 (s, 2H), 3.77 (t, J = 6.2 Hz, 2H), 3.92 (t, J = 6.4 Hz, 2H), 4.20 (t, J = 6.4 Hz, 2H), 6.74–6.83 (m, 4H), 7.00–7.96 (m, 13H). A stirred solution of this compound (0.46 g, 0.75 mmol) and diethylamine (0.32 mL, 3.0 mmol) was refluxed in toluene (100 mL) for 20 h in the presence of a catalytic amount of NaI. The mixture was washed with water (3 × 25 mL), then with brine (3 × 25 mL). The organic layer was collected and dried over Na₂SO₄. The solvent was removed and the residue was purified by flash chromatography (toluene/acetone 20:80), affording **14** as a yellow oil (0.04 g, 9%). ¹H NMR δ: 1.10 (t, J = 6.4 Hz, 6H), 1.18–1.62 (m, 8H), 1.63–1.85 (m, 2H), 2.19 (s, 3H), 2.32–2.43 (m, 2H), 2.58–2.71 (m, 4H), 2.89 (t, J = 6.4 Hz, 2H), 3.53 (s, 2H), 3.91 (t, J = 6.2 Hz, 2H), 4.08 (t, J = 6.4 Hz, 2H), 6.74–6.83 (m, 4H), 7.00–7.96 (m, 13H). ES-MS *m/z*: 647 (M + 1). Anal. C₄₂H₅₀N₂O₄ (C, H, N).

6.1.15. (2-{4-[7-(Benzylmethylamino)heptyloxy]phenyl}benzofuran-3-yl)-[4-(2-chloroethoxy)phenyl]methanone (**15**)

Using the previous procedure and starting from **2** [11] (0.62 g, 1.45 mmol) and 4-(2-chloroethoxy)benzoyl chloride (0.38 g, 1.7 mmol), (2-{4-[7-(benzylmethylamino)heptyloxy]phenyl}benzofuran-3-yl)-[4-(2-chloroethoxy)phenyl]methanone was obtained as a dark yellow oil (0.53 g, 60%). ¹H NMR δ: 1.17–1.59 (m, 8H), 1.56–1.79 (m, 2H), 2.15 (s, 3H), 2.32–2.39 (m, 2H), 3.47 (s, 2H), 3.81 (t, J = 6.2 Hz, 2H), 3.89 (t, J = 6.4 Hz, 2H), 4.21 (t, J = 6.4 Hz, 2H), 6.72–6.87 (m, 4H), 7.05–8.02 (m, 13H). Using the previous procedure and starting from (2-{4-[7-(benzylmethylamino)heptyloxy]phenyl}benzofuran-3-yl)-[3-(2-chloroethoxy)phenyl]methanone (0.46 g, 0.75 mmol), **15** was obtained as a yellow oil (0.03 g, 8%). ¹H NMR δ: 1.02–1.12 (m, 6H), 1.17–1.61 (m, 8H), 1.62–1.86 (m, 2H), 2.21 (s, 3H), 2.35–2.46 (m, 2H), 2.60–2.73 (m, 4H), 2.80–2.92 (m, 2H), 3.55 (s, 2H), 3.93 (t, J = 6.2 Hz, 2H), 4.05 (t, J = 6.4 Hz, 2H), 6.75–6.86 (m, 4H), 7.00–7.94 (m, 13H). ES-MS *m/z*: 647 (M + 1). Anal. C₄₂H₅₀N₂O₄ (C, H, N).

6.1.16. (2-{4-[7-(Benzylmethylamino)heptyloxy]phenyl}benzofuran-3-yl)-[4-(2-morpholinoethoxy)phenyl]methanone (**16**)

(2-{4-[7-(benzylmethylamino)heptyloxy]phenyl}benzofuran-3-yl)-[4-(2-chloroethoxy)phenyl]methanone (0.4 g, 0.57 mmol) and morpholine (0.1 g, 1.14 mmol), were refluxed in toluene for 20 h in the presence of NaI. The mixture was washed with water (3 × 25 mL), then with brine (3 × 25 mL). The organic layer was collected and dried over Na₂SO₄. The solvent was removed and the residue was purified by flash chromatography (toluene/acetone 20:80), affording **16** as a yellow oil (0.08 g, 21%). ¹H NMR δ: 1.21–1.58 (m, 8H), 1.62–1.83 (m, 2H), 2.20 (s, 3H), 2.30–2.42 (m, 2H), 2.56–2.62 (m, 4H), 2.73–2.83 (m, 2H), 3.43 (s, 2H), 3.65–3.80 (m, 4H), 3.93 (t, J = 6.3 Hz, 2H), 4.13 (t, J = 6.2 Hz, 2H), 6.81 (d, J = 8.4 Hz, 2H), 7.12–7.41 (m, 10H), 7.50–7.62 (m, 4H), 7.83–7.95 (m, 2H). ES-MS *m/z*: 661 (M + 1). Anal. C₄₂H₄₈N₂O₅ (C, H, N).

6.1.17. General procedure for the synthesis of compounds **32–36**

SnCl₄ (1.2 eq.) was added dropwise to a mixture of **28** (1 eq.) and the selected acylchloride (1.2 eq.) in dry dichloromethane and the resulting solution was stirred at room temperature overnight. The reaction was quenched with ice/water and stirred for 1 h. The organic layer was separated and the aqueous one was extracted with dichloromethane. The combined organic extracts were dried (Na₂SO₄), filtered and concentrated under reduced pressure to afford the desired 3-acylated benzofurans (**32–36**), generally as honey coloured oils purified by flash chromatography.

6.1.17.1. {2-[4-(7-Bromoheptyloxy)phenyl]benzofuran-3-yl}naphthalen-1-yl-methanone (**32**). (0.06 g, 16%). (petroleum ether/ethyl acetate 98:02). ¹H NMR δ: 1.25–1.58 (m, 6H), 1.62–1.95 (m, 4H),

3.41 (t, $J = 6.6$ Hz, 2H), 3.86 (t, $J = 6.6$ Hz, 2H), 6.60–6.64 (m, 2H), 7.20–7.38 (m, 4H), 7.50–7.65 (m, 7H), 7.84–7.90 (m, 2H), 8.55–8.60 (m, 1H).

6.1.17.2. *{2-[4-(7-Bromoheptyloxy)phenyl]benzofuran-3-yl}naphthalen-2-yl-methanone (33)*. (0.16 g, 47%). (petroleum ether/ethyl acetate 98:02). $^1\text{H NMR } \delta$: 1.29–1.56 (m, 6H), 1.64–1.92 (m, 4H), 3.40 (t, $J = 6.6$ Hz, 2H), 3.86 (t, $J = 6.6$ Hz, 2H), 6.73–6.78 (m, 2H), 7.21–7.38 (m, 3H), 7.42–7.63 (m, 4H), 7.64–7.90 (m, 4H), 7.95–8.01 (m, 1H), 8.34 (s, 1H).

6.1.17.3. *Biphenyl-4-yl-{2-[4-(7-bromoheptyloxy)phenyl]benzofuran-3-yl}methanone (34)*. (0.22 g, 58%). (petroleum ether/ethyl acetate 98:02). $^1\text{H NMR } \delta$: 1.27–1.58 (m, 6H), 1.62–1.95 (m, 4H), 3.39 (t, $J = 6.6$ Hz, 2H), 3.90 (t, $J = 6.6$ Hz, 2H), 6.78–6.82 (dd, $J_1 = 2.2$ Hz, $J_2 = 8.4$ Hz, 2H), 7.24–7.50 (m, 5H), 7.51–7.71 (m, 8H), 7.90–7.93 (m, 2H).

6.1.17.4. *Anthracen-9-yl-{2-[4-(7-bromoheptyloxy)phenyl]benzofuran-3-yl}methanone (35)*. (0.08 g, 18%). (petroleum ether/ethyl acetate 98:02). $^1\text{H NMR } \delta$: 1.31–1.61 (m, 6H), 1.62–1.95 (m, 4H), 3.43 (t, $J = 6.6$ Hz, 2H), 3.80 (t, $J = 6.2$ Hz, 2H), 6.29 (br, 2H), 6.72–7.82 (m, 10H), 7.84–8.12 (m, 4H), 8.34 (s, 1H).

6.1.17.5. *{2-[4-(7-bromoheptyloxy)phenyl]benzofuran-3-yl}-p-tolylmethanone (36)*. (0.26 g, 62%). (petroleum ether/ethyl acetate 98:2). $^1\text{H NMR } \delta$: 1.41–1.59 (m, 6H), 1.70–1.95 (m, 4H), 2.28 (s, 3H), 3.42 (t, $J = 6.6$ Hz, 2H), 3.81 (t, $J = 6.6$ Hz, 2H), 6.81–6.87 (m, 1H), 7.14–7.40 (m, 7H), 7.56–7.67 (m, 4H).

6.1.18. General procedure for the synthesis of compounds 37–44

SnCl_4 (1.2 eq.) was added dropwise to a mixture of **31** (1 eq.) and the selected acylchloride (1.2 eq.) in dry dichloromethane and the resulting solution was stirred at room temperature overnight. The reaction was quenched with ice/water and stirred for 1 h. The organic layer was separated and the aqueous one was extracted with dichloromethane. The combined organic extracts were dried (Na_2SO_4), filtered and concentrated under reduced pressure to afford the desired 3-acylated benzofurans (**37–44**), generally as honey coloured oils purified by flash chromatography.

6.1.18.1. *{2-[3-(7-Bromoheptyloxy)phenyl]benzofuran-3-yl}phenylmethanone (37)*. (0.09 g, 28%). (petroleum ether/ethyl acetate 98:2). $^1\text{H NMR } \delta$: 1.25–1.58 (m, 6H), 1.62–1.95 (m, 4H), 3.38 (t, $J = 6.6$ Hz, 2H), 3.83 (t, $J = 6.2$ Hz, 2H), 6.85 (dt, $J_1 = 1.8$ Hz, $J_2 = 8.4$ Hz, 1H), 7.11–7.40 (m, 7H), 7.47–7.58 (m, 2H), 7.78 (d, $J = 8.0$ Hz, 2H).

6.1.18.2. *{2-[3-(7-Bromoheptyloxy)phenyl]benzofuran-3-yl}-m-tolylmethanone (38)*. (0.06 g, 18%). (petroleum ether/ethyl acetate 98:2). $^1\text{H NMR } \delta$: 1.41–1.59 (m, 6H), 1.70–1.95 (m, 4H), 2.28 (s, 3H), 3.42 (t, $J = 6.6$ Hz, 2H), 3.81 (t, $J = 6.6$ Hz, 2H), 6.81–6.87 (m, 1H), 7.14–7.40 (m, 7H), 7.56–7.67 (m, 4H).

6.1.18.3. *{2-[3-(7-Bromoheptyloxy)phenyl]benzofuran-3-yl}-p-tolylmethanone (39)*. (0.09 g, 27%). (petroleum ether/ethyl acetate 98:2). $^1\text{H NMR } \delta$: 1.25–1.58 (m, 6H), 1.62–1.95 (m, 4H), 2.36 (s, 3H), 3.40 (t, $J = 6.6$ Hz, 2H), 3.82 (t, $J = 6.2$ Hz, 2H), 6.84 (dt, $J_1 = 1.8$ Hz, $J_2 = 8.6$ Hz, 1H), 7.12–7.38 (m, 7H), 7.48–7.59 (m, 2H), 7.77 (d, $J = 8.0$ Hz, 2H).

6.1.18.4. *{2-[3-(7-Bromoheptyloxy)phenyl]benzofuran-3-yl}-2-methoxyphenylmethanone (40)*. (0.2 g, 59%). (petroleum ether/ethyl acetate 94:6). $^1\text{H NMR } \delta$: 1.42–1.58 (m, 6H), 1.62–1.98 (m, 4H), 3.41 (t, $J = 6.6$ Hz, 2H), 3.55 (s, 3H), 3.84 (t, $J = 6.2$ Hz, 2H), 6.69 (d,

$J = 8.4$ Hz, 1H), 6.84–6.92 (m, 2H), 7.12–7.38 (m, 6H), 7.45–7.56 (m, 2H), 7.73–7.78 (m, 1H).

6.1.18.5. *{2-[3-(7-Bromoheptyloxy)phenyl]benzofuran-3-yl}-3-methoxyphenylmethanone (41)*. (0.07 g, 21%). (petroleum ether/ethyl acetate 98:2). $^1\text{H NMR } \delta$: 1.40–1.58 (m, 6H), 1.60–1.95 (m, 4H), 3.42 (t, $J = 6.6$ Hz, 2H), 3.73 (s, 3H), 3.81 (t, $J = 6.2$ Hz, 2H), 6.82–6.88 (m, 1H), 7.01–7.06 (m, 1H), 7.15–7.41 (m, 8H), 7.56–7.62 (m, 2H).

6.1.18.6. *2-[3-(7-Bromoheptyloxy)phenyl]benzofuran-3-yl}-2,3-dimethoxyphenylmethanone (42)*. (0.17 g, 47%). (petroleum ether/ethyl acetate 90:10). $^1\text{H NMR } \delta$: 1.42–1.51 (m, 6H), 1.72–1.92 (m, 4H), 3.40 (t, $J = 6.6$ Hz, 2H), 3.74 (s, 3H), 3.82 (s, 3H), 3.91 (t, $J = 6.6$ Hz, 2H), 6.81–6.93 (m, 4H), 7.13–7.40 (m, 5H), 7.51–7.65 (m, 2H).

6.1.18.7. *{2-[3-(7-Bromoheptyloxy)phenyl]benzofuran-3-yl}-3,4-dimethoxyphenylmethanone (43)*. (0.13 g, 36%). (petroleum ether/ethyl acetate 90:10). $^1\text{H NMR } \delta$: 1.30–1.56 (m, 6H), 1.60–1.98 (m, 4H), 3.40 (t, $J = 6.6$ Hz, 2H), 3.80–3.90 (m, 8H), 6.72–6.88 (m, 2H), 7.16–7.59 (m, 9H).

6.1.18.8. *{2-[3-(7-Bromoheptyloxy)phenyl]benzofuran-3-yl}-3,5-dimethoxyphenylmethanone (44)*. (0.07 g, 16%). (petroleum ether/ethyl acetate 90:10). $^1\text{H NMR } \delta$: 1.41–1.58 (m, 6H), 1.62–1.95 (m, 4H), 3.41 (t, $J = 6.6$ Hz, 2H), 3.68 (s, 6H), 3.81 (t, $J = 6.2$ Hz, 2H), 6.56–6.58 (m, 1H), 6.83–6.90 (m, 1H), 6.98 (s, 1H), 6.99 (s, 1H), 7.13–7.41 (m, 5H), 7.56–7.66 (m, 2H).

6.1.19. General procedure for the synthesis of compounds 8–11, 18–25

A stirred solution of opportune compounds **32–35**, **37–44** (1 eq.) and *N*-benzyl-*N*-methylamine (2 eq.) in toluene was refluxed for 48 h. The mixture was washed with water. The organic layer was dried over Na_2SO_4 and the solvent was removed. The residue was purified by flash chromatography (toluene/acetone 98:2) to afford **8–11**, **18–25** generally as yellowish oil.

6.1.19.1. *(2-{4-[7-(Benzylmethylamino)heptyloxy]phenyl}benzofuran-3-yl)naphthalen-1-yl-methanone (8)*. (0.04 g, 62%). $^1\text{H NMR } \delta$: 1.21–1.62 (m, 8H), 1.63–1.79 (m, 2H), 2.18 (s, 3H), 2.35 (t, $J = 6.2$ Hz, 2H), 3.47 (s, 2H), 3.84 (t, $J = 6.6$ Hz, 2H), 6.59–6.64 (m, 2H), 7.16–7.35 (m, 8H), 7.52–7.63 (m, 7H), 7.85 (d, $J = 8.2$ Hz, 2H), 8.57 (d, $J = 8.2$ Hz, 1H). ES-MS m/z : 582 ($M + 1$). Anal. $\text{C}_{40}\text{H}_{39}\text{NO}_3$ (C, H, N).

6.1.19.2. *(2-{4-[7-(Benzylmethylamino)heptyloxy]phenyl}benzofuran-3-yl)naphthalen-2-yl-methanone (9)*. (0.17 g, 99%). $^1\text{H NMR } \delta$: 1.25–1.60 (m, 8H), 1.64–1.80 (m, 2H), 2.18 (s, 3H), 2.35 (t, $J = 6.4$ Hz, 2H), 3.48 (s, 2H), 3.84 (t, $J = 6.6$ Hz, 2H), 6.75 (d, $J = 8.8$ Hz, 2H), 7.18–7.38 (m, 8H), 7.41–7.85 (m, 8H), 7.96–8.02 (m, 1H), 8.33 (s, 1H). ES-MS m/z : 582 ($M + 1$). Anal. $\text{C}_{40}\text{H}_{39}\text{NO}_3$ (C, H, N).

6.1.19.3. *(2-{4-[7-(Benzylmethylamino)heptyloxy]phenyl}benzofuran-3-yl)biphenyl-4-yl-methanone (10)*. (0.18 g, 73%). $^1\text{H NMR } \delta$: 1.21–1.62 (m, 8H), 1.64–1.80 (m, 2H), 2.20 (s, 3H), 2.40 (t, $J = 6.4$ Hz, 2H), 3.50 (s, 2H), 3.90 (t, $J = 6.6$ Hz, 2H), 6.80 (d, $J = 8.8$ Hz, 2H), 7.19–7.45 (m, 11H), 7.54–7.68 (m, 7H), 7.91 (d, $J = 8.2$ Hz, 2H). ES-MS m/z : 608 ($M + 1$). Anal. $\text{C}_{42}\text{H}_{41}\text{NO}_3$ (C, H, N).

6.1.19.4. *Anthracen-9-yl-(2-{4-[7-(benzylmethylamino)heptyloxy]phenyl}benzofuran-3-yl)methanone (11)*. (0.06 g, 70%). $^1\text{H NMR } \delta$: 1.25–1.62 (m, 8H), 1.64–1.80 (m, 2H), 2.22 (s, 3H), 2.40 (t, $J = 6.4$ Hz, 2H), 3.52 (s, 2H), 3.79 (t, $J = 6.6$ Hz, 2H), 6.18–6.40 (m, 2H), 7.25–7.52 (m, 15H), 7.89–7.93 (m, 4H), 8.34 (s, 1H). ES-MS m/z : 632 ($M + 1$). Anal. $\text{C}_{44}\text{H}_{41}\text{NO}_3$ (C, H, N).

6.1.19.5. (2-{3-[7-(Benzylmethylamino)heptyloxy]phenyl}benzofuran-3-yl)phenylmethanone (**18**). (0.09 g, 65%). $^1\text{H NMR } \delta$: 1.21–1.62 (m, 8H), 1.63–1.79 (m, 2H), 2.18 (s, 3H), 2.35 (t, $J = 6.4$ Hz, 2H), 3.47 (s, 2H), 3.84 (t, $J = 6.6$ Hz, 2H), 6.89–6.94 (m, 1H), 7.16–7.62 (m, 15H), 7.80–7.93 (m, 2H). ES-MS m/z : 532 ($M + 1$). Anal. $\text{C}_{36}\text{H}_{37}\text{NO}_3$ (C, H, N).

6.1.19.6. (2-{3-[7-(Benzylmethylamino)heptyloxy]phenyl}benzofuran-3-yl)-*p*-tolylmethanone (**19**). (0.05 g, 77%). $^1\text{H NMR } \delta$: 1.22–1.62 (m, 8H), 1.64–1.80 (m, 2H), 2.20 (s, 3H), 2.28 (s, 3H), 2.37 (t, $J = 6.4$ Hz, 2H), 3.50 (s, 2H), 3.80 (t, $J = 6.6$ Hz, 2H), 6.84 (d, $J = 8.2$ Hz, 1H), 7.16–7.42 (m, 12H), 7.56–7.67 (m, 4H). ES-MS m/z : 546 ($M + 1$). Anal. $\text{C}_{37}\text{H}_{39}\text{NO}_3$ (C, H, N).

6.1.19.7. (2-{3-[7-(Benzylmethylamino)heptyloxy]phenyl}benzofuran-3-yl)-*p*-tolylmethanone (**20**). (0.08 g, 82%). $^1\text{H NMR } \delta$: 1.25–1.62 (m, 8H), 1.64–1.80 (m, 2H), 2.19 (s, 3H), 2.35–2.40 (m, 5H), 3.48 (s, 2H), 3.80 (t, $J = 6.6$ Hz, 2H), 6.82–6.86 (m, 1H), 7.11–7.42 (m, 12H), 7.54 (t, $J = 8.8$ Hz, 2H), 7.77 (d, $J = 8.8$ Hz, 2H). ES-MS m/z : 546 ($M + 1$). Anal. $\text{C}_{37}\text{H}_{39}\text{NO}_3$ (C, H, N).

6.1.19.8. (2-{3-[7-(Benzylmethylamino)heptyloxy]phenyl}benzofuran-3-yl)-2-methoxyphenylmethanone (**21**). (0.15 g, 70%). $^1\text{H NMR } \delta$: 1.28–1.62 (m, 8H), 1.65–1.82 (m, 2H), 2.19 (s, 3H), 2.37 (t, $J = 6.6$ Hz, 2H), 3.48 (s, 2H), 3.53 (s, 3H), 3.84 (t, $J = 6.6$ Hz, 2H), 6.68 (d, $J = 8.0$ Hz, 1H), 6.80–6.91 (m, 2H), 7.10–7.35 (m, 11H), 7.44–7.55 (m, 2H), 7.75–7.80 (m, 1H). ES-MS m/z : 562 ($M + 1$). Anal. $\text{C}_{37}\text{H}_{39}\text{NO}_4$ (C, H, N).

6.1.19.9. (2-{3-[7-(Benzylmethylamino)heptyloxy]phenyl}benzofuran-3-yl)-3-methoxyphenylmethanone (**22**). (0.05 g, 66%). $^1\text{H NMR } (\text{CDCl}_3) \delta$: 1.25–1.61 (m, 8H), 1.65–1.82 (m, 2H), 2.20 (s, 3H), 2.38 (t, $J = 6.4$ Hz, 2H), 3.49 (s, 2H), 3.73 (s, 3H), 3.81 (t, $J = 6.2$ Hz, 2H), 6.83–6.87 (m, 1H), 6.98–7.05 (m, 1H), 7.16–7.20 (m, 2H), 7.22–7.32 (m, 8H), 7.37–7.41 (m, 3H), 7.56–7.63 (m, 2H). ES-MS m/z : 562 ($M + 1$). Anal. $\text{C}_{37}\text{H}_{39}\text{NO}_4$ (C, H, N).

6.1.19.10. (2-{3-[7-(Benzylmethylamino)heptyloxy]phenyl}benzofuran-3-yl)-2,3-dimethoxyphenyl methanone (**23**). (0.14 g, 77%). $^1\text{H NMR } \delta$: 1.27–1.61 (m, 8H), 1.65–1.83 (m, 2H), 2.18 (s, 3H), 2.36 (t, $J = 6.6$ Hz, 2H), 3.48 (s, 2H), 3.73 (s, 3H), 3.79 (s, 3H), 3.90 (t, $J = 6.6$ Hz, 2H), 6.80–6.95 (m, 4H), 7.12–7.34 (m, 10H), 7.51–7.55 (m, 1H), 7.63–7.68 (m, 1H). ES-MS m/z : 592 ($M + 1$). Anal. $\text{C}_{38}\text{H}_{41}\text{NO}_5$ (C, H, N).

6.1.19.11. (2-{3-[7-(Benzylmethylamino)heptyloxy]phenyl}benzofuran-3-yl)-3,4-dimethoxyphenyl methanone (**24**). (0.09 g, 65%). $^1\text{H NMR } \delta$: 1.25–1.62 (m, 8H), 1.69–1.80 (m, 2H), 2.20 (s, 3H), 2.37 (t, $J = 6.6$ Hz, 2H), 3.49 (s, 2H), 3.80–3.89 (m, 8H), 6.74 (d, $J = 8.6$ Hz, 1H), 6.83–6.88 (m, 1H), 7.23–7.39 (m, 10H), 7.43–7.60 (m, 4H). ES-MS m/z : 592 ($M + 1$). Anal. $\text{C}_{38}\text{H}_{41}\text{NO}_5$ (C, H, N).

6.1.19.12. (2-{3-[7-(Benzylmethylamino)heptyloxy]phenyl}benzofuran-3-yl)-3,5-dimethoxyphenyl methanone (**25**). (0.05 g, 67%). $^1\text{H NMR } \delta$: 1.25–1.61 (m, 8H), 1.64–1.81 (m, 2H), 2.20 (s, 3H), 2.38 (t, $J = 6.6$ Hz, 2H), 3.50 (s, 2H), 3.67 (s, 6H), 3.80 (t, $J = 6.2$ Hz, 2H), 6.57 (s, 1H), 6.84–6.88 (m, 1H), 6.98 (d, $J = 8.2$ Hz, 2H), 7.14–7.41 (m, 10H), 7.56–7.67 (m, 2H). ES-MS m/z : 592 ($M + 1$). Anal. $\text{C}_{38}\text{H}_{41}\text{NO}_5$ (C, H, N).

6.1.20. [2-(4-[7-[(3-Hydroxybenzyl)methylamino]heptyloxy]phenyl)benzofuran-3-yl]-*p*-tolylmethanone (**45**)

A stirred solution of **36** (0.7 g, 1.38 mmol) and 3-methylaminomethylphenol (0.38 g, 2.77 mmol) in toluene (120 mL) was refluxed for 20 h. The mixture was washed with water, the

organic layer was dried over Na_2SO_4 and the solvent was removed. The residue was purified by flash chromatography (toluene/acetone 90:10), to afford **45** as a yellowish oil (0.16 g, 21%). $^1\text{H NMR } \delta$: 1.20–1.60 (m, 8H), 1.62–1.83 (m, 2H), 2.19 (s, 3H), 2.23–2.41 (m, 5H), 3.42 (s, 2H), 3.83–3.97 (m, 2H), 6.63–6.87 (m, 4H), 7.11–7.38 (m, 6H), 7.39–7.58 (m, 2H), 7.62–7.81 (m, 4H).

6.1.21. Methylcarbamic acid 3-[[methyl-(7-{4-[3-(4-methylbenzoyl)benzofuran-2-yl]phenoxy}heptyl)-amino]methyl]phenyl ester (**17**)

To a solution of **45** (0.1 g, 0.18 mmol) in CH_2Cl_2 , NaH (0.004 g, 0.18 mmol) and methyl isocyanate (0.010 g, 0.18 mmol) were added. The mixture was stirred for 24 h, then quenched with ice/water and extracted with CH_2Cl_2 . The organic layer was dried and evaporated. The crude was purified by flash chromatography (toluene/acetone 60:40), affording **17** as a clear oil (0.06 g, 54%). $^1\text{H NMR } \delta$: 1.21–1.59 (m, 8H), 1.63–1.82 (m, 2H), 2.18 (s, 3H), 2.23–2.41 (m, 5H), 2.82 (s, 3H), 3.45 (s, 2H), 3.83–3.97 (m, 2H), 4.91–5.02 (br, 1H), 6.62–6.85 (m, 4H), 7.09–7.41 (m, 6H), 7.47–7.59 (m, 2H), 7.61–7.84 (m, 4H). ES-MS m/z : 619 ($M + 1$). Anal. $\text{C}_{39}\text{H}_{42}\text{N}_2\text{O}_5$ (C, H, N).

6.2. Biological evaluation methods

6.2.1. Inhibition of AChE and BuChE

The capacity of **3–25** to inhibit hAChE activity was assessed using the Ellman's method [14]. Compounds **1** and **2**, galantamine, tacrine and rivastigmine were used as reference compounds. Initial rate assays were performed at 37 °C with a Jasco V-530 double beam spectrophotometer. Stock solutions of the tested compound (1 mM) were prepared in methanol and diluted in methanol. The assay solution consisted of a 0.1 M phosphate buffer, pH 8.0, with the addition of 340 μM 5,5'-dithiobis(2-nitrobenzoic acid), 0.02 unit/mL human recombinant AChE or human serum BuChE (Sigma Chemical, St. Louis, MO), and 550 μM substrate (acetylthiocholine iodide or butyrylthiocholine iodide, respectively). Assay solutions with and without inhibitor were preincubated at 37 °C for 20 min followed by the addition of substrate. Blank solutions containing all components except AChE or BuChE were prepared in parallel to account for the non-enzymatic hydrolysis of the substrate. Five increasing concentrations of the inhibitor were used, able to give an inhibition of the enzymatic activity in the range of 20–80%. The results were plotted by placing the percentage of inhibition in function of the decimal log of the final inhibitor concentration. Linear regression and IC_{50} values were calculated using Microcal Origin 3.5 software (Microcal Software, Inc).

6.2.2. Inhibition of β -amyloid aggregation

6.2.2.1. Preparation of solutions. Stock solution of 1 μM was prepared by solubilizing the lyophilized $\text{A}\beta_{25-35}$ peptide by brief vortexing in sterile water at 4 °C, then by sonication for 1 min. The peptide stock solution was aliquoted and stored at –20 °C. All steps were carried out at 4 °C to prevent $\text{A}\beta_{25-35}$ polymerization. The new compounds were solubilized in MeOH solution to a concentration of 1 M. The stock solution was diluted to obtain aliquots with concentrations between 0.1 and 50 μM , then stored at –20 °C.

6.2.3. Measurement of inhibitory activity by UV–visible spectroscopy

To study the kinetic of $\text{A}\beta_{25-35}$ polymerization alone, experiments were carried out by using a reaction mixture containing 80 μL phosphate buffer (10 mM final concentration) and 10 μL $\text{A}\beta_{25-35}$ (100 μM final concentration), pH 7.2. When $\text{A}\beta_{25-35}$ was added to the buffer solution, we performed sonication for 1 min to avoid any peptide aggregation. 10 μL MeOH were added to the solution to have the same conditions for the experiments with the new compounds. To study the inhibitory activity of the new compounds, experiments were carried out by using a reaction

mixture containing 80 μL phosphate buffer (10 mM final concentration), 10 μL MeOH containing 10 μM final concentration of one of the new compounds or 10 μL MeOH containing 0.1, 1, 10, 20 and 50 μM final concentration for IC_{50} determination and 10 μL $\text{A}\beta_{25-35}$ (100 μM final concentration), pH 7.2. All steps were carried out at 4 $^{\circ}\text{C}$ to prevent $\text{A}\beta_{25-35}$ polymerization. UV–visible spectroscopy was performed on a Cary 300 bio UV–visible spectrophotometer. Polymerization kinetics were monitored in the range of 190–380 nm between 0 and 6 h. For each inhibition experiment, one sample containing $\text{A}\beta_{25-35}$ alone, another containing the new compound alone and a third with curcumin as inhibitor reference were used in parallel as controls in the same experimental conditions. Moreover, to rule out any influence due to the new compounds absorbance, their UV–visible spectra were subtracted from the $\text{A}\beta_{25-35}$ absorption spectra. At least three independent measurements were made for all cases. All results are presented with means and standard deviation. IC_{50} was calculated by using a least-square fitting technique to match the experimental data with a sigmoidal curve. IC_{50} was the concentration of the new compound inhibiting the formation of $\text{A}\beta$ fibrils to 50% of the control value.

6.2.4. The neuroprotective effects against $\text{A}\beta_{25-35}$ peptide

6.2.4.1. Chemicals. $\text{A}\beta_{25-35}$ peptide, 3-(4,5-dimethyl-2-thiazolyl)-2,5-diphenyl-2H-tetrazolium bromide (MTT), dihydroethidium (DHE) and Congo red (CR) were purchased from Sigma Chemical Co. All other reagents were of the highest grade of purity commercially available.

6.2.4.2. $\text{A}\beta_{25-35}$ peptide preparation for neurotoxicity assay. $\text{A}\beta_{25-35}$ peptide was dissolved in hexafluoroisopropanol (HFIP) to 1 mg/mL, sonicated and incubated at room temperature for 24 h to produce unaggregated $\text{A}\beta$ peptide. The HFIP was dried under vacuum in a Speed Vac and the resulting peptide film was dissolved in DMSO to 1 mM. The unaggregated $\text{A}\beta_{25-35}$ stock solution was then aliquoted and stored at -20°C until use. For various biological assay, the $\text{A}\beta_{25-35}$ stock solution was diluted directly into cell culture media.

6.2.4.3. Cell culture. Human neuronal SH–SY5Y cells were routinely grown at 37 $^{\circ}\text{C}$ in a humidified incubator with 5% CO_2 in Dulbecco's modified Eagle's medium supplemented with 10% foetal bovine serum, 2 mM glutamine, 50 U/mL penicillin and 50 $\mu\text{g}/\text{mL}$ streptomycin.

6.2.4.4. Determination of $\text{A}\beta_{25-35}$ peptide-induced neurotoxicity. To evaluate the protective effects of compounds against $\text{A}\beta_{25-35}$ peptide induced neurotoxicity, the SH–SY5Y cells were seeded in 96-well plates at 3×10^4 cells/well, incubated for 24 h and subsequently treated with 10 μM of unaggregated $\text{A}\beta_{25-35}$ peptide for 3 h at 37 $^{\circ}\text{C}$ in 5% CO_2 , in presence or absence of various concentrations of compounds (1–30 μM). The neuronal viability in terms of mitochondrial metabolic function was evaluated by the reduction of MTT to formazan as previously described [18]. The cellular reduction of MTT represents an indicator of the initial events underlying the mechanism of $\text{A}\beta_{25-35}$ peptide neurotoxicity. Briefly, after removal of the treatment, SH–SY5Y cells were washed with phosphate buffered saline (PBS) and incubated with MTT (5 mg/mL) in PBS for 2 h at 37 $^{\circ}\text{C}$ in 5% CO_2 . After further washing, the formazan crystals were dissolved with isopropanol. The amount of formazan was measured (570 nm, ref. 690 nm) with a spectrophotometer (TECAN[®], GENios, Salzburg, Austria). The neuronal viability was expressed as a percentage of control cells and calculated by the formula: (absorbance of treated neurons/absorbance of untreated neurons) \times 100.

6.2.4.5. Determination of $\text{A}\beta_{25-35}$ peptide binding to the cell surface. SH–SY5Y cells were seeded in 96-well plates at 5×10^3 cells/well for 24 h. At the end of incubation, the medium was changed with a fresh one with $\text{A}\beta_{25-35}$ peptide (10 μM) and various compounds (30 μM) for 10, 20 and 30 min and then washed twice with PBS. The residual $\text{A}\beta_{25-35}$ peptide cell complex was stained with CR in PBS for 20 min and measured with a spectrophotometer (TECAN[®], GENios) at 540 nm (bound CR). CR values were reported as percent increases in treated cells vs. untreated cells (taken as 100%).

6.2.4.6. Determination of $\text{A}\beta_{25-35}$ peptide-induced intracellular ROS formation. ROS formation was determined using the fluorescent probe DHE ($\lambda_{\text{excitation}} = 380$ nm, $\lambda_{\text{emission}} = 445$ nm). SH–SY5Y cells were cultured in BD Falcon[™] 8-well Culture slides (surface area 0.7 cm^2/well) at 1×10^4 cells/well for 24 h. At the end of incubation, SH–SY5Y cells were washed and incubated with DHE (10 μM) for 15 min in the dark. After removal of the probe, cells were washed with PBS and incubated with DMEM serum free for 1 h at 37 $^{\circ}\text{C}$. Intracellular ROS formation was measured under a fluorescence microscope (Zeiss Axio Imager M1). Fluorescence images were captured with an AxioVision image recording system computer. Four randomly selected areas with 50–100 cells in each were analysed and the values obtained are expressed as fold increases of ROS vs. untreated cells.

6.2.5. Binding studies to CB receptors

Membranes from HEK-293 cells stably transfected with the human recombinant CB1 receptor ($B_{\text{max}} = 2.5$ pmol/mg protein) or the human recombinant CB2 receptor ($B_{\text{max}} = 4.7$ pmol/mg protein) were incubated with [³H]-CP-55, 940 (0.14 nM/ $K_d = 0.18$ nM and 0.084 nM/ $K_d = 0.31$ nM respectively for CB1 and CB2 receptor) as the high affinity ligand and displaced with 10 μM WIN 55212-2 as the heterologous competitor to measure non-specific binding (K_i values 9.2 nM and 2.1 nM respectively for CB1 and CB2 receptor). All compounds were tested following the procedure described by the manufacturer (Perkin Elmer, Italia). Displacement curves were generated by incubating membranes with [³H]-CP-55, 940 and increasing concentrations of test compounds for 90 min at 30 $^{\circ}\text{C}$. K_i values were calculated by applying the Cheng–Prusoff equation to the IC_{50} values (obtained by GraphPad) for the displacement of the bound radioligand by increasing concentrations of the test compounds. Data are reported as means of at least $n = 3$ experiments.

6.2.6. Statistical analysis

Data are reported as mean \pm SD of at least 3 independent experiments. Statistical analysis was performed using one-way ANOVA with Dunnett post hoc test and Student's *t*-test, as appropriate. Pearson's test was also used to assess correlation. Differences were considered significant at $p < 0.05$. Analyses were performed using PRISM 3 software on a Windows platform.

References

- [1] C. Ballard, S. Gauthier, A. Corbett, C. Brayne, D. Aarsland, E. Jones, Alzheimer's disease, *Lancet* 377 (2011) 1019–1031.
- [2] A.V. Terry, J.J. Buccafusco, The cholinergic hypothesis of age and Alzheimer's disease-related cognitive deficits: recent challenges and their implications for novel drug development, *J. Pharmacol. Exp. Ther.* 306 (2003) 821–827.
- [3] C.L. Masters, D.J. Selkoe, Biochemistry of amyloid β -protein and amyloid deposits in Alzheimer disease, *Cold Spring Harb. Perspect. Med.* 2 (2012) a006262.
- [4] M. Jin, N. Shepardson, T. Yang, G. Chen, D. Walsh, D.J. Selkoe, Soluble amyloid β -protein dimers isolated from Alzheimer cortex directly induce Tau hyperphosphorylation and neuritic degeneration, *Proc. Natl. Acad. Sci. U. S. A.* 108 (2011) 5819–5824.

- [5] S. Darvesh, D.A. Hopkins, C. Geula, Neurobiology of butyrylcholinesterase, *Nat. Rev. Neurosci.* 4 (2003) 131–138.
- [6] N.H. Greig, T. Utsuki, D.K. Ingram, Y. Wang, G. Pepeu, C. Scali, Q.S. Yu, J. Mamczarz, H.W. Holloway, T. Giordano, D. Chen, K. Furukawa, K. Sambamurti, A. Brossi, D.K. Lahir, Selective butyrylcholinesterase inhibition elevates brain acetylcholine, augments learning and lowers Alzheimer beta-amyloid peptide in rodent, *Proc. Natl. Acad. Sci. U. S. A.* 102 (2005) 17213–17218.
- [7] T. Bisogno, V. Di Marzo, The role of the endocannabinoid system in Alzheimer's disease: facts and hypotheses, *Curr. Pharm. Des.* 14 (2008) 2299–3305.
- [8] T. Bisogno, V. Di Marzo, Cannabinoid receptors and endocannabinoids: role in neuroinflammatory and neurodegenerative disorders, *CNS Neurol. Disord. Drug Targets* 9 (2010) 564–573.
- [9] R. Morphy, Z. Rankovic, Designing multiple ligands – medicinal chemistry strategies and challenges, *Curr. Pharm. Des.* 15 (2009) 587–600.
- [10] A. Cavalli, M.L. Bolognesi, A. Minarini, M. Rosini, V. Tumiatti, M. Recanatini, C. Melchiorre, Multi-target-directed ligands to combat neurodegenerative diseases, *J. Med. Chem.* 51 (2008) 347–372.
- [11] S. Rizzo, C. Rivière, L. Piazza, A. Bisi, S. Gobbi, M. Bartolini, V. Andrisano, F. Morroni, A. Tarozzi, J.P. Monti, A. Rampa, Benzofuran-based hybrid compounds for the inhibition of cholinesterase activity, β amyloid aggregation, and A β neurotoxicity, *J. Med. Chem.* 51 (2008) 2883–2886.
- [12] C.C. Felder, K.E. Joyce, E.M. Briley, M. Glass, K.P. Mackie, K.J. Fahey, G.J. Cullinan, D.C. Hunden, D.W. Johnson, M.O. Chaney, G.A. Koppel, M. Brownstein, LY320135, a novel cannabinoid CB1 receptor antagonist, unmasks coupling of the CB1 receptor to stimulation of cAMP accumulation, *J. Pharmacol. Exp. Ther.* 284 (1998) 291–297.
- [13] S. Rizzo, A. Bisi, M. Bartolini, F. Mancini, F. Belluti, S. Gobbi, V. Andrisano, A. Rampa, Multi-target strategy to address Alzheimer's disease: design, synthesis and biological evaluation of new tacrine-based dimers, *Eur. J. Med. Chem.* 46 (2011) 4336–4343.
- [14] G.L. Ellman, K.D. Courtney, V. Andres, R.M. Featherstone, A new rapid colorimetric determination of acetylcholinesterase activity, *Biochem. Pharmacol.* 7 (1961) 88–95.
- [15] C. Rivière, T. Richard, L. Quentin, S. Krisa, J.-M. Mérillon, J.-P. Monti, Inhibitory activity of stilbenes on Alzheimer's β -amyloid fibrils *in vitro*, *Bioorg. Med. Chem.* 15 (2007) 1160–1167.
- [16] A. Klegeris, D.G. Walker, P.L. McGeer, Activation of macrophages by Alzheimer beta amyloid peptide, *Biochem. Biophys. Res. Commun.* 199 (1994) 984–991.
- [17] C.J. Pike, A.J. Walencewicz-Wasserman, J. Kosmoski, D.H. Cribbs, C.G. Glabe, C.W. Cotman, Structure-activity analyses of beta-amyloid peptides: contributions of the beta 25–35 region to aggregation and neurotoxicity, *J. Neurochem.* 64 (1995) 253–265.
- [18] K. Ono, K. Hasegawa, H. Naiki, M. Yamada, Curcumin has potent anti-amyloidogenic effects for Alzheimer's beta-amyloid fibrils *in vitro*, *J. Neurosci. Res.* 75 (2004) 742–750.
- [19] A. Tarozzi, F. Morroni, A. Merlicco, C. Bolondi, G. Teti, M. Falconi, G. Cantelli-Forti, P. Hrelia, Neuroprotective effects of cyanidin 3-O-glucopyranoside on amyloid beta (25–35) oligomer-induced toxicity, *Neurosci. Lett.* 473 (2010) 72–76.
- [20] J. Wilhelm, R. Vytásek, I. Ostádalová, L. Vajner, Evaluation of different methods detecting intracellular generation of free radicals, *Mol. Cell. Biochem.* 328 (2009) 167–176.
- [21] A. Rampa, A. Bisi, P. Valenti, M. Recanatini, A. Cavalli, V. Andrisano, V. Cavrini, L. Fin, A. Burianni, P. Giusti, Acetylcholinesterase inhibitors: synthesis and structure-activity relationships of ω -[N-methyl-N-(3-alkylcarbamoyloxyphenyl)methyl]-aminoalkoxyheteroaryl derivatives, *J. Med. Chem.* 41 (1998) 3976–3986.
- [22] A. Rampa, L. Piazza, F. Belluti, S. Gobbi, A. Bisi, M. Bartolini, V. Andrisano, V. Cavrini, A. Cavalli, M. Recanatini, P. Valenti, Acetylcholinesterase inhibitors: SAR and kinetic studies on ω -[N-methyl-N-(3-alkylcarbamoyloxyphenyl)-methyl]-aminoalkoxyaryl derivatives, *J. Med. Chem.* 44 (2001) 3810–3820.
- [23] M. Mesulam, A. Guillozet, P. Shaw, B. Quinn, Widely spread butyrylcholinesterase can hydrolyze acetylcholine in the normal and Alzheimer brain, *Neurobiol. Dis.* 9 (2002) 88–93.
- [24] Y. Furukawa-Hibi, T. Alkam, A. Nitta, A. Matsuyama, H. Mizoguchi, K. Suzuki, S. Moussaoui, Q.S. Yu, N.H. Greig, T. Nagai, K. Yamada, Butyrylcholinesterase inhibitors ameliorate cognitive dysfunction induced by amyloid- β peptide in mice, *Behav. Brain Res.* 225 (2011) 222–229.
- [25] D.J. Selkoe, Soluble oligomers of the amyloid beta-protein impair synaptic plasticity and behavior, *Behav. Brain Res.* 192 (2008) 106–113.
- [26] L. Wicklund, R.N. Leao, A.M. Stromberg, M. Mousavi, O. Hovatta, A. Nordberg, A. Marutle, Beta-amyloid 1–42 oligomers impair function of human embryonic stem cell-derived forebrain cholinergic neurons, *PLoS One* 5 (2010) e15600.
- [27] M. Bartolini, V. Andrisano, Strategies for the inhibition of protein aggregation in human diseases, *ChemBiochem* 11 (2010) 1018–1035.
- [28] A.S. Johansson, J. Bergquist, C. Volbracht, A. Päiviö, M. Leist, L. Lannfelt, A. Westlind-Danielsson, Attenuated amyloid-beta aggregation and neurotoxicity owing to methionine oxidation, *Neuroreport* 18 (2007) 559–563.
- [29] M.E. Clementi, S. Marini, M. Coletta, F. Orsini, B. Giardina, F. Misiati, Abeta(31–35) and Abeta(25–35) fragments of amyloid beta-protein induce cellular death through apoptotic signals: role of the redox state of methionine-35, *FEBS Lett.* 579 (2005) 2913–2918.
- [30] C.G. Glabe, Common mechanisms of amyloid oligomer pathogenesis in degenerative disease, *Neurobiol. Aging* 27 (2006) 570–575.
- [31] A. Rauk, Why is the amyloid beta peptide of Alzheimer's disease neurotoxic? *Dalton Trans.* 14 (2008) 1273–1282.
- [32] M. Bjerke, E. Portelius, L. Minthon, A. Wallin, H. Anckarsater, R. Anckarsater, N. Andreasen, H. Zetterberg, U. Andreasson, K. Blennow, Confounding factors influencing amyloid beta concentration in cerebrospinal fluid, *Int. J. Alzheimers Dis.* (2010) 986310.
- [33] M.S. Garcia-Ayllon, I. Riba-Llena, C. Serra-Basante, J. Alom, R. Boopathy, J. Saez-Valero, Altered levels of acetylcholinesterase in Alzheimer plasma, *PLoS One* 5 (2010) e8701.
- [34] B.S. Harvey, K.S. Ohlsson, J.L. Määg, I.F. Musgrave, S.D. Smid, Contrasting protective effects of cannabinoids against oxidative stress and amyloid- β evoked neurotoxicity *in vitro*, *Neurotoxicology* 33 (2012) 138–146.
- [35] P. Marini, A.S. Moriello, L. Cristino, M. Palmery, L. De Petrocellis, V. Di Marzo, Cannabinoid CB1 receptor elevation of intracellular calcium in neuroblastoma SH-SY5Y cells: interactions with muscarinic and delta-opioid receptors, *Biochim. Biophys. Acta* 1793 (2009) 1289–1303.
- [36] M. Haghani, M. Shabani, M. Javan, F. Motamedi, M. Janahmadi, CB1 cannabinoid receptor activation rescues amyloid β -induced alterations in behaviour and intrinsic electrophysiological properties of rat hippocampal CA1 pyramidal neurons, *Cell. Physiol. Biochem.* 29 (2012) 391–406.
- [37] M.L. Bolognesi, R. Banzi, M. Bartolini, A. Cavalli, A. Tarozzi, V. Andrisano, A. Minarini, M. Rosini, V. Tumiatti, C. Bergamini, R. Fato, G. Lenaz, P. Hrelia, A. Cattaneo, M. Recanatini, C. Melchiorre, Novel class of quinone-bearing polyamines as multi-target-directed ligands to combat Alzheimer's disease, *J. Med. Chem.* 50 (2007) 4882–4897.